2010

Effect of catalyst preparation conditions on the performance of eggshell cobalt/SiO2 catalysts for Fischer-Tropsch synthesis

Syed Ali Z. H Gardezi
University of South Florida

Effect of Catalyst Preparation Conditions on the Performance of Eggshell Cobalt/SiO_2 Catalysts for Fischer-Tropsch Synthesis

by

Syed Ali Z. H. Gardezi

A thesis submitted in partial fulfillment
of the requirements for the degree of
Master of Science in Chemical Engineering
Department of Chemical and Biomedical Engineering
College of Engineering
University of South Florida

Co-Major Professor: John T. Wolan, Ph.D.
Co-Major Professor: Babu Joseph, Ph.D.
Vinay K. Gupta, Ph.D.

Date of Approval:
June 28, 2010

Keywords: silica, calcination, fixed bed reactor, biomass, diesel, aviation fuel, conversion, selectivity

Dedication

First and foremost, I want to dedicate my research to the energy deprived nations of this world, I sincerely hope that it will contribute to the expansion of the alternate energy sector, and reduce the dependence on depleting fossil resources, resulting in the preservation of mother earth and its inhabitants.

I would also like to dedicate this research to the friendly and loving people of the United States who have made me feel at home. I am optimistic that my research will play a definite role in achieving the goal of energy independence and will help create more domestic jobs.

Acknowledgements

Above all, I am heartily thankful for the patience, guidance and helpful ideas of my principal adviser, Dr. John T. Wolan, not to mention his support in allaying of my fears that arose during the course of my graduate school experience. The good advice, and friendship of my second advisor, Dr Babu Joseph, has been invaluable on both an academic and a personal level, for which I am extremely grateful. I would also like to thank my committee member, Dr. Vinay K. Gupta for his "eye opening" suggestions.

The expertise of Dr. Sesha Srinivasan from the Clean Energy Research Center, with regard to hydrogen chemisorption experiments came in very handy. I am thankful to Haitao "Eddie" Li of the USF Green Energy Systems Lab for his help with the BET measurements in this work, and Bijith Mankidy for his help with procuring the TPR results.

I would also like to acknowledge my lab partners, current and former: Ala'a Kababji, Chris Monteparo, Brad Ridder, William Bosshart, Sandra Pettit, and Lucky Roy Landrgan. Their words of encouragement, intelligent conversations, and helpful advice are a memorable part of my graduate school experience.

Last, but by no means least, I want to thank my wife Arusa Aleen Gardezi for her constant support. Like a guardian angel, she stands by my side and appeases me whenever I am in dire strait.

Table of Contents

List of Tables

List of Figures

Effect of Catalyst Preparation Conditions on the Performance of Eggshell Cobalt/SiO_2 Catalysts for Fischer-Tropsch Synthesis

Syed Ali Z. H. Gardezi

Abstract

A highly selective eggshell Fischer-Tropsch catalyst has been fabricated via interaction of hydrophobic and hydrophilic molecules on thermally treated silica gel. The physical interactions of the mesoporous silica support and the effect of catalyst preparation conditions on the performance of the cobalt/SiO_2 were explored. It was found that dispersion and performance of the FT cobalt/SiO_2 catalyst were significantly affected by the preparation technique used. In this study we focus on two key variables: the solvent used during the precursor loading and the calcination atmosphere. Silanol groups on the silica surface and near-surface regions can alter morphology and dispersion of the supported active metals. Solvents used for precursor such as water or alcohol attach to these silanol sites in specific configurations and compete with metal salts during ion exchange and adsorption. By fine tuning the solvent attachments on heat treated silica we have fabricated a cobalt/silica catalyst with high dispersion and low metal loads. Additionally, since silica has affinity for both polar and non-polar molecule depending on the surface conditions; this property has been exploited in preparing an engineered eggshell profile. This together with simultaneous calcination/ reduction in a dynamic hydrogen environment has been shown to further enhance dispersion and reducibility. Characterization techniques including BET, XPS, XRD, H-chemisorption and FTIR were employed. Catalyst activity, product selectivity, distribution and conversion were studied using a bench scale fixed bed reactor fitted with a GC/MS instrument.

Chapter 1: Introduction

The demand for clean transportation fuel continues to grow at an ever increasing pace while limited supplies of fossil continues to increase the fuel prices. Projected trends show that production of crude oil will peak around 2030, while, the global energy requirement is expected to rise by 60% [1]. Concerns about global warming are putting pressure on developing renewable sources for transportation fuel. Raw materials like biomass, coal, natural gas, and even municipal waste can be converted to clean fuel via a thermo-chemical route called Fischer-Tropsch synthesis (FTS), a catalytic route employing transition metals such as Fe, Co and Ru. FTS converts hydrogen and carbon monoxide on a catalyst as per following nominal reaction [2]:

$$nCO + (2n+1)\,H_2 \longrightarrow C_nH_{2n+2} + nH_2O$$

where "n" can be anywhere from 1(methane) to 30 or higher (waxes). Exploration of this chemistry by experimental and theoretical techniques reveals that ruthenium, cobalt and iron are the catalysts of choice for FTS [3]. The cobalt catalyst has some additional benefits e.g. lower water gas shift activity, higher per pass conversion, low rate of attrition, and production of more paraffinic hydrocarbons [4]. Ruthenium has the highest activity, but is not commercially used because of its high cost and limited availability. When compared to cobalt and ruthenium, iron has the lowest cost but produces more waxes and olefins; iron also promotes the undesirable water gas shift reaction.

The active catalyst metal is usually deposited on an inert support material like silica, alumina, titania, silicon carbide etc. Although inactive to the reactant gases, these supports can affect the overall synthesis by controlling the morphology of the active catalytic specie, its dispersion, and metal-support interactions. Silica and alumina

supports are most commonly used due to the strength and porous nature of the material. Alumina, when used as support, decreases the reducibility of the catalyst [4]. Silica, on the other hand does not appreciably produce irreducible compounds, however, the active metal dispersion is lower than that for alumina [4]. Iglesia et al. [5] showed that for large metal particles (above 7 nm) the reaction rate is proportional to the cobalt surface sites (i.e. dispersion). Dispersion of a silica supported catalyst can be improved by the addition of noble metals (Rh, Ru, Pt and Pd). These metals also facilitate the reduction of the metal oxides; however, cost is a limiting factor. Surface wetting of silica with different polar solvents (ethanol, 1 propanol and 1 butanol) is another method in practice to increase metal distribution [6]. For an active Co catalyst, CoO and Co_3O_4 are the desired phase because they easily reduce to cobalt metal [4]. Synthesis of the active catalyst requires strong interaction between the metal and the support; however, if too strong, these interactions can lead to formation of irreducible mixed metal support oxides. Ho et al. [7] observed that the use of ethanol as a solvent (instead of water) for a cobalt nitrate precursor resulted in metal support interaction of sufficient strength to increase active metal dispersion while retaining a high extent of reduction.

A silica surface has affinity for both polar and non-polar molecule depending on surface conditions. This property was exploited in this study in order to prepare an effective eggshell catalyst. Different polar molecules have different attachment patterns on the silica surface, thus by controlling the surface condition one can control the dispersion on silica supported particles. The solvent used during catalyst preparation also affects the deposition of the salt precursor via ion exchange.

Thermal treatment of the catalyst precursor (drying, calcinations and reduction) also impacts the dispersion. The calcination atmosphere changes the arrangement of the surface molecules to some degree and affects the metal support interaction. Earnest et al. [8] showed that during the reduction process the reaction of CoO and SiO_2 results in the formation of irreducible cobalt ortho-silicates. This formation of silicates increases the dispersion.

This research work is focused on the development of a highly active, selective, tunable and economic Co/SiO_2 Fischer-Tropsch catalyst. To this end the following hypotheses are presented (i) silica surface possess both hydrophilic and hydrophobic properties depending on the pretreatment conditions (ii) presence of water on silica surface reduces active metal dispersion (iii) eggshell catalyst profile ensure tune-ability depending on the thickness of shell (iv) space velocity plays primary role during thermal treatment of catalyst precursor.

In order to assist the reader, this thesis is organized as follows. Prior research work is discussed in Chapter 2 in order to identify shortcomings, areas of improvement and direction of this study. The experimental strategy used in this work as a result of these findings has been laid out in Chapter 3. Final preparation of representative samples is presented in Chapter 4. Theoretical comparison and verification of the hypotheses via several characterization techniques is presented in Chapter 5. Evaluation and discussion of sample performance under actual FTS conditions in a fixed bed reactor is given in Chapter 6. Based on these results a theory has been developed and presented in Chapter 7 together with future studies.

Chapter 2: Background

2.1 Silica Structure

Much controversy exists regarding the nature of silica surface. Fundamental studies by Stober [9], Meyer and Heckerman [10], and Bering and Serpinski [11] indicate that a silica surface mainly consists of siloxane network in the bulk while hydroxyl groups are attached on to the "Si" surface atoms. However these groups are not similar to each other in adsorption or reaction behavior. Figure 2 represents a general arrangement on a silica surface. Belyakova et al.[12] identifies that the number of hydroxyl (silanol) groups on different type of silica surfaces are the same i.e. 4 -5 SiOH groups per nm^2. Lange [13] states that water associates with these silanol groups in two ways, by hydrogen bonding and physically adsorption. Dalton and Iler [14] state that there is at least a monolayer of water immobilized on the surface silanol groups due to hydrogen bonding under normal conditions. This "glassy layer" tends to shield the underlying silica network from foreign species. Klier and Zettlemoyer [15] suggest that water sits "oxygen down" on the silanol groups. De Boer and Vleeskens [16] argue that the silica loses this adsorbed water at around 120 ^{o}C in ambient air, unless it is present in micropores, where the loss is at 180^{o}C. Drying under a vacuum, at low temperature is also an effective technique to remove all the surface adsorbed water. Armistead and Hockey [17] found that removal of the silanol group takes place around 400-450 ^{o}C in ambient air where half of the hydroxyl groups leave the silica surface creating large siloxane areas that do not rehydrate readily. Young and Bush [18] suggest that the siloxane network is essentially hydrophobic in nature, and it excessively slows down rehydration.

Whenever a silica gel is loaded with an active metal under ambient condition it is not possible to have strong surface-metal interaction because of the presence of a stagnant

single or double aqueous layer. In order to obtain sufficiently strong metal-support interaction the silica surface must be dried at 200 ^{o}C or above prior to metal loading. Under ambient conditions, silica gel only attaches polar molecules to its surface. In order to make use of the polar-non polar system in tandem, the silica surface has to be heated to 500-600 ^{o}C, thus exposing the hydrophobic siloxane space while retaining sufficient "polar regions".

2.2 Silica–Solvent Interaction

On fully hydroxylated silica surfaces, water first covers all silanol groups via multiple hydrogen bonding. This creates one or at most two layers of water in equilibrium with the surface. The key to this strong attachment is the inherent nature of the strong electron donor water which attaches itself with the vicinal, isolated and even mutual hydrogen bonded silanol group. For organic compounds (e.g. ethanol), Hair et al. [19] as well as Clark-Monks and Ellis [20] claim that the best adsorption sites are the freely vibrating isolated silanol groups and there is little tendency of bonding on the mutually hydrogen bonded adjacent SiOH. Robert [21] finds that ethanol is adsorbed vertically oriented on the hydroxyl group (hydrogen bonded to the OH groups of silanol). Furthermore, the number of alcohol molecules esterified on the silica surface depended on the size of the carbon chain and branching [22]. Around 3.7 ethoxy groups per nm^2 attach on the surface leaving some silanol sites unoccupied [23].

Figure 3 and 5 illustrates the differing attachment of water and ethanol molecules on a silica surface. Due to the strong affinity of water towards the surface, it is not possible for a solute molecule to anchor directly on the silica base; rather an immobile aqua monolayer will form as shown in Figure 4. It is also possible that this monolayer is already present on the gel due to the hygroscopic nature of silica. On the other hand, alcohol due to its vertical orientation can lead to random distribution of vertical stacks on isolated silanol groups. The gaps between these stacks present ideal location for solute anchorage on the silica surface. Due to steric hindrance, not every silica atom reacts with

an alkoxy group, so the concentration of ethoxy groups can be less than predicted i.e. 3.7 per nm^2.

2.3 Silica-Solute Interaction in an Aqueous System

For the case of a dilute aqueous solution, a classical model using the Nernest equation describes the interaction of solute ions with a silica surface [24]. According to this model a solute ion when in the vicinity of the surface, diffuses into a "double layer" of ions which are kept in motion due to thermal phonons. Then a significant number of these ions based on their size enter the "stern layer", a compact immobilized layer near the surface.

Healy et al. [25] have performed pioneering work on the state of precipitated cobalt ions and possible interaction with a silica surface. At low pH (6 or below) in low salt concentrations, the active specie is Co^{2+}, swarming in a diffuse double layer (kept in motion by thermal phonons). At a pH of approximately 6.5 but well below the complete precipitation limit the aqueous salt near the surface is able to anchor; the interaction takes following form.

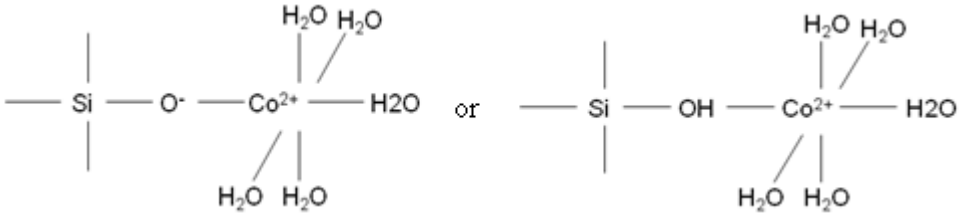

Figure 1. The interaction between the metal and the support in the intermediate pH range

Upon precipitation (i.e. pH =8) the adsorbed species exist in the form of polymeric chain of cobalt (II) hydroxide and it covers entire surface. This branched chain also consists of anions and water molecules. Rajamathi and Kamath [26] state that the composition of this specie depends on the temperature. At around 80°C in an aqueous system a hydrotalcite-type structure is obtained having the formula $Co(OH)_2(NO_3)_{0.27}$ .2/3 H_2O. While close to 100°C it takes the form $Co(OH)_{1.75}(NO_3)_{0.25}$ .2/3 H_2O.

During the precipitation process, if the pH of the support surface is above its isoelectric point, the direct contact between salt ions and the surface is possible. However, these salt ions can attach in many different forms depending on the precipitation process. In the case of a well mixed, fully precipitated system a polymeric chain may attach to the support surface, otherwise the hydrated ions of Co^{2+} will be in close proximity to the silica. These ions may remain in thermal motion or attach to the support surface.

2.4 Silica-Solute Interaction in a Non-Aqueous System

Generally, it is believed that an inorganic salt dissolved in an organic solvent can be adsorbed on a silica surface [27]. For silica gel the order of the adsorption is as follows, alcohol > salt ions > acetone. Russell et al. [27] state that the addition of a small amount of water (2-3%) increases the adsorption. They also ascertain that adsorption is preferred over ion exchange. Dugger et al. [28] suggest that alkali metal nitrates dissolved in ethanol react slightly with the surface of silica gel. However, when higher alcohols are used which concentrate the silanol by their hydrogen bonding (large width and branch number)) no adsorption is observed. For this reason, ethanol was used in this study.

Adsorption sites for the salt and alcohol are the polar silanol groups on the silica surface, as shown in Figure 5. Alcohol is not adsorbed on all silanol groups (only half of the available silanol groups are covered), however, alcohol is more preferentially adsorbed than salt. The strong contact between salt and support requires a strong attractive force i.e. negative silanol site (SiO^-) attracting positive cobalt ions (Co^{2+}). It seems that around 3% by weight of water in salt-alcohol solution can cause enough ionization required to renders sufficient negative charge to the silica surface. This promotes ion exchange between salt and silica resulting in coordination bonding between them. Under these circumstances, the anchorage of salt on the silica surface will be random and far apart, reducing the possibility of agglomeration. Also, for substantial loading, silica gel has to be in contact with a very concentrated salt-alcohol solution to avoid the formation of the stagnant aqua layer by excess water molecules.

2.5 Calcination Atmosphere

Thermal treatment (calcination) of the catalyst precursor controls the final distribution of active metal. During calcination it is necessary to provide an environment conducive for smooth precursor decomposition to avoid sintering and to ensure high dispersion of the active metal. Other important parameters include the control of heating rate, an atmosphere that retards crystal growth, and flow rates that ensure swift removal of heat treatment product. Despite its importance, there is lack of constructive research in this area.

2.6 Impact of Water in Calcination Atmosphere

Borg et al. [29] identify that under identical dynamic conditions, the presence or absence of steam in air impacts the active metal's crystal size and the amount of residual nitrates in the final product. They concluded that the decomposition of cobalt nitrate leads to the formation of water. If water is already present in the calcination atmosphere, then the decomposition product cannot be easily removed. The long residence time of water on the surface favors crystal growth. Puskas et al. [30] state that water reacts with cobalt oxide on catalyst surface to form a hydroxide. Cobalt hydroxide further reacts with migrating silicic acid to form hard to reduce silicates which are inactive in Fischer-Tropsch Synthesis.

$$CoO + H_2O \longrightarrow Co(OH)_2$$

$$Co(OH)_2 + SiO(OH)_2 \longrightarrow CoSiO_3 + 2H_2O$$

The equilibrium concentration of water regardless of the atmosphere seems to be the primary factor that controls the catalyst properties. However, claims are controversial. It appears that the presence of water during precursor decomposition is detrimental; it gives rise to mixed metal-support oxide and decreases the extent of catalyst reduction. On the other hand, there are claims that support the formation of agglomerated species, and indicate a significant reduction in metal support interaction in the presence of moist air.

2.7 Impact of Oxygen Scavengers in Calcination Atmosphere

Sietsma et al. [33] argue that the presence of NO/He in the calcination atmosphere leads to a gradual decomposition of the nitrate precursor following zero order kinetics. These results were confirmed by thermal and kinetic analysis. According to Sietsma, a sudden surge in endothermic heat transfer is observed during calcination in the static air. The inert NO/He environment improves repartition of the active metal on the support. Similarly, Linyang et al. [34] identify that the presence of nitrogen during calcination leads to improved segregation between the active metal and added promoter. This can enhance the interaction between the active metal and the underlying support. Borg et al. [29] observe that the presence of a dynamic nitrogen atmosphere improves the metal dispersion and its precursor decomposition.

Puskas et al. [30] provides an alternate explanation about the impact of thermal treatment in a reducing atmosphere. Here, cobalt silicate is formed during calcination in a reducing or inert environment. The formation of water and metal hydroxides during the reduction process (or in an inert atmosphere) provides a low potential energy pathway for the development of ortho as well as meta-silicates. He also states that the space velocity of the calcination gas plays an important role in controlling the reaction equilibrium during cobalt silicate formation.

There exists a great deal of controversy over the possible advantages and disadvantages of thermal treatment using oxygen scavenging gases. Some claim that under the scavenging environment the heat flux over the surface is gradual; this avoids thermal sintering of metal particles [33]. The surface rearrangement also leads to more segregation between the particles and more contact with the support. While others state that if the space velocity of the gases is kept low, there is no advantage of using scavenging or reducing atmosphere as the product water will eventually give rise to a moist atmosphere [30]. It appears that the flow rate of calcination gases control the final properties of active catalyst, for favorable results, the flow rate should be kept as high as possible.

2.8 Impact of Dynamic Atmosphere

Borg et al. [29] have compared the properties of a Co/SiO_2 catalyst prepared under dynamic nitrogen and dynamic air. They are of the view that ambient air with a higher flow rate allows a smaller particle size distribution when compared to an inert atmosphere at low flow. Sietsma et al. [33] have found that as the gas hourly space velocity of NO is increased during calcination, the average crystal size of a NiO/SiO_2 catalyst system is reduced. In conclusion the degree of size reduction varies with the GHSV i.e. at low velocities the variation is the highest.

2.9 Impact of Calcination Temperature

The purpose of high temperature calcination is to decompose the precursor to oxide states; however there are certain factors that must be addressed. Borg et al. [29] have shown that the cobalt crystal size increases with increasing the temperature of calcinations from 400 to 700 ^oC due to sintering of metal crystallites. The observed catalyst TPR profile shows a shift to a higher metal support interaction when the calcination temperature is increased. Conversely Coulter and Sault [34] observed the formation of metal-support oxides at low temperatures under vacuum annealing. Jablonski et al. [35] state that calcination around 800-900 ^oC (either in argon or oxygen) results in the decomposition of Co_3O_4 to CoO which further leads to the reaction between CoO and SiO_2 forming cobalt silicate. These cobalt silicates are only partially reducible at high temperature (600 ^oC). Kababji et al. [31] state that high calcination temperature approximately 500 ^oC leads to the loss in surface area due to silica migration. Tao et al. [36] have reported that a slow calcinations temperature ramp rate of 0.5-2 ^oC/min ensures superior textural properties of silica supported cobalt catalysts.

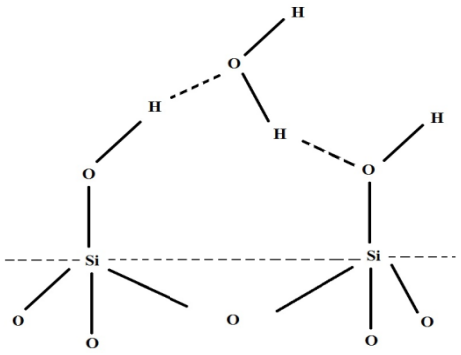

Figure 2. A schematic represenation of silica surface showing silanol group and hydrogen bonded water molecule

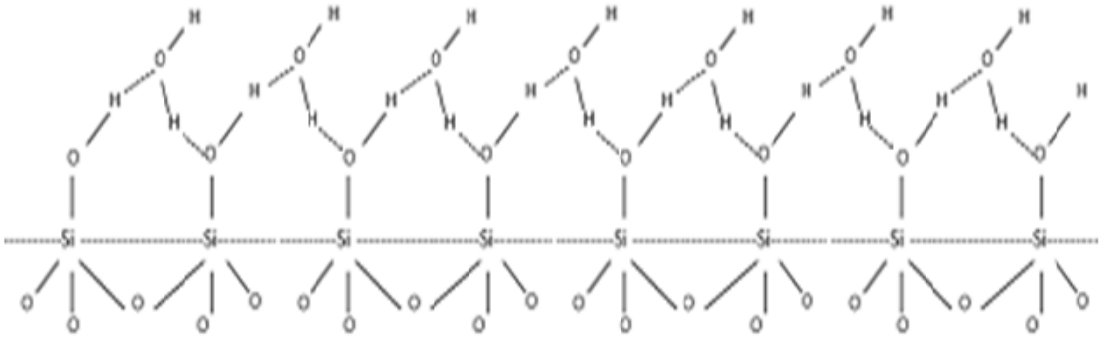

Figure 3. Silica surface surrounded by water molecule via multiple bonding

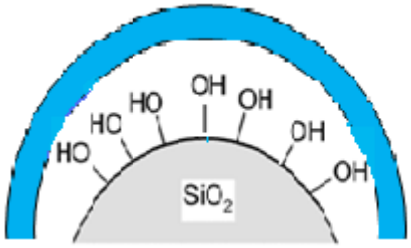

Figure 4. Immobilized single/multiple aqueous layer surrounding silanol groups

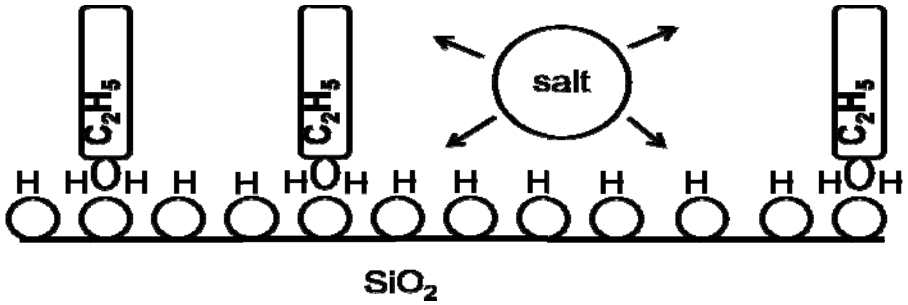

Figure 5. Vertical stacking of alcohol (ethanol) allowing direct contact between the salt and the support

2.10 Catalyst Morphology

Iglesia et al. [37] has argued that Fischer-Tropsch synthesis is diffusion limited process and the activity of the catalyst depends on the arrival of reactants, and the removal of products from the active sites. Post et al. [38] showed that eggshell catalyst pellets of 2mm decouple the diffusion limitation from other reactor constraints e.g. pressure drop. Peluso et al. [39] have shown that an eggshell catalyst with 10% cobalt within the half radius of a 1.81 mm catalyst gives higher middle distillate selectivity. Iglesia et al. [40] have shown that 1-3 mm diameter pellets are required to control pressure gradients across a packed bed reactor; however, to reach desired conversion with these particles reactor volume has to be very large. According to Iglesia, this limitation can be overcome by using an eggshell catalyst design. To this end, Iglesia has defined a parameter "χ" which is dependent on certain catalyst characteristics. Based on their modeling results, this parameter can be used to determine the optimum thickness required in an eggshell catalyst to maximize activity.

2.11 Conclusion

It is evident that silica gel possesses both the hydrophobic and the hydrophilic properties depending on the temperature and environment. This provides a unique opportunity to tailor interactions on the silica support based on specific catalytic requirements. Also within a certain class of solvents, the pattern of attachment with the silica surface varies appreciably. This phenomenon affects the uptake (loading) of solute and its interaction with the silica surface. Thus, the final properties of the loaded catalyst depend on the type and proportion of the solvents used.

There is controversy over the preferable conditions leading to smooth precursor decomposition. The role of inert calcination environment is not sufficiently understood. The resultant effect of water on the catalyst surface is still under debate. The impact of gas space velocity during calcination requires more investigation. The surface-gas interactions during the calcination are not known.

In this study, the role of calcination environment (inert and oxygenated) will be investigated. It appears that the space velocity (of the calcination gas) is the primary factor that controls the surface properties after thermal treatment. On the other hand, the calcination environment may control the kinetics of decomposition. Also there is a possibility that calcination gas interferes with the surface atoms resulting in segregation of active metal atoms. All these factors require a thorough investigation in order to gain a strong insight into the thermal decomposition process.

The "eggshell" profile ensures high catalyst activity and product selectivity. However, the optimum eggshell thickness has not yet been defined clearly. Much of the prior work is based on the single phase modeling during the Fischer-Tropsch reaction. The experimental evidence required to establish a general correlation between the selectivity and the eggshell thickness is not available. These controversies and lack of specific data presents an extensive opportunity of research in order to prove a direct correlation between the product selectivity, catalyst surface properties and eggshell thickness.

Chapter 3: Design of Experiments

The design of experiments presented in this work is based on a fish bone analysis shown in Figure 6. From this analysis a matrix of possible experiments has been developed using Taguchi design [41].

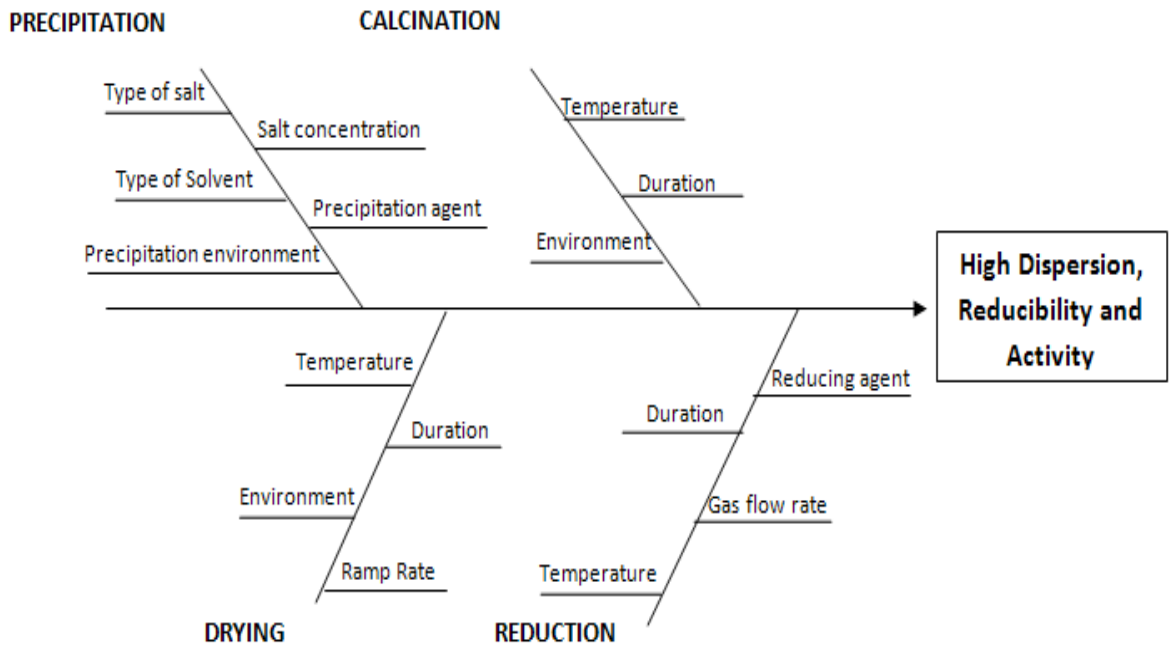

Figure 6. Fish Bone analysis of catalyst preparation conditions

Prior work indicates that the catalyst activity follows the order; $Co_2(CO)_8$ > $Co(NO3)_2$ > $Co(CH_3COO)_2$ while chain growth probability follows the sequence $Co(NO_3)_2$ > $Co_2(CO)_8$ > $Co(CH_3COO)_2$ [42]. Based on these findings $Co(NO_3)_2$ is a preferred precursor salt. The salt concentration is based on the solubility in water (134 g/100 ml) and ethanol (9 g/100 mL). Typically a base is used as the precipitation agent for this system. Urea was chosen in this case due to rapid precipitation and slow hydrolysis [43] resulting in high dispersion.

The choice of the solvent is governed by the desire to develop an eggshell profile. The interactions of polar and non-polar molecules with the silica surface and their mutual repulsion provide a novel path to develop the eggshell profile. Ethanol is the preferred polar solvent due to its unique surface attachment and its relative short chain length, which leads to lesser overall branching on the silica surface. The solvent n-heptane was selected as a non polar solvent because it has not been cited in the literature for use in FTS catalyst synthesis.

The drying rate is adjusted to ensure the stability of egg shell profile. It has been reported that at low rate, drying proceeds slowly down the pores, thus concentrating the precursor towards the center of the pellets. However, if the drying rate is too fast, deposition occurs near the entrance [44]. Thus, the more rapid the evaporation, the greater is the chance of eggshell formation. Drying in a vacuum furnace, already heated to the drying temperature i.e. $100^{o}C$, can successfully achieve rapid drying.

For a given catalyst sample, the TPR (temperature program reduction) spectra indicates the optimum temperature range for the reduction process. TPR also indicates the presence of different phases during the reduction process and the optimum rate of reduction. The rate of reduction controls the attachment of cobalt on the silica; yet Ernst et al. [8] attribute this fixation to the reaction of CoO with silica to form Co_2SiO_4 during the reduction as shown below.

$$2\ CoO + SiO_2 \longrightarrow Co_2SiO_4$$

Activity is the primary indicator of catalyst effectiveness. However, as shown in the "Fish Bone", the activity depends on the loading of the catalyst, active metal distribution (dispersion) and percentage reduction. The objective is to choose the catalyst preparation and pre-treatment condition to achieve higher dispersion while maintaining the appreciable degree of reduction. Other properties like accessibility to catalyst sites (pore size distribution) and surface area have to be kept within acceptable limits. Keeping in

mind these constraints and our area of interest, following variables (Table 1) influence the dispersion and the reducibility of the supported catalyst.

Table 1. Important variables that influence catalyst properties

Variable	Lower value (-1)	Central value (0)	Upper value (+1)
Precipitation Solvent (PrSl)	Alcohol	Alcohol (1-2% water)	Water
Precipitation Environment (PrEv)	Nitrogen	Dry Air	Moist Air
Drying/Calcination rate (DrClRt)	Slow	Nominal	Rapid
Calcination Environment (CalEv)	Hydrogen	Nitrogen	Static Moist Air
Reduction rate (RdRt)	1 K/min	5 K/min	20 K/min

The scope of this study has been limited to the parameters hypothesized to have the strongest impact on activity and selectivity of the catalyst system. As stated earlier the factors that greatly influence the catalyst preparation and pre-treatment include: (i) the choice of solvent during precursor loading, and, (ii) the thermal treatment of the precursor. These two areas have not yet been studied in tandem. Thus, the overall object of this work is to identify their relative impact on the final properties of Co/SiO_2 eggshell catalyst for FTS.

Based on these findings, the final set of experiments are limited to the impact of changes in precursor solvent and calcination environment (experiment 2, 5, 10 and 17 in Table 2). These experiments (shown in Table 3) will be used to understand various aspects leading to the desired catalytic properties of high selectivity and activity. The results of this study will not only add to the knowledge base but also lead to the development of catalyst with superior properties.

In a broader prospective this work compares the situation where water was present in any form (solvent or moisture in atmosphere) to that where no water exists.

Table 2. Matrix of experiments

Experiment	PrSl	PrEv	DrClRt	CalEv	RdRt
1	-1	-1	-1	-1	-1
2	-1	-1	+1	-1	-1
3	-1	-1	-1	+1	-1
4	-1	-1	+1	-1	+1
5	-1	-1	+1	+1	-1
6	-1	+1	-1	-1	-1
7	-1	+1	-1	+1	-1
8	-1	+1	+1	-1	+1
9	-1	+1	+1	+1	+1
10	+1	+1	+1	-1	-1
11	+1	-1	-1	-1	+1
12	+1	-1	-1	+1	+1
13	+1	-1	+1	-1	-1
14	+1	-1	+1	+1	-1
15	+1	+1	-1	-1	+1
16	+1	+1	-1	+1	+1
17	+1	+1	+1	+1	-1
18	+1	+1	+1	+1	+1

Table 3. Reduced set of variables

Catalyst ID	Precipitation		Calcination		Area of Investigation
	Base/Solvent	Environment	(K) / hr	Environment	
Sample -1	Urea/ Water	Ambient Air	623/16	Air	Change in solvent and precipitation
Sample-2	Urea/ Ethanol	Nitrogen	623/16	Air	Change in Calcination environment
Sample-3	Urea/ Ethanol	Nitrogen	623/16	Hydrogen	Change in solvent and precipitation environment
Sample-4	Urea/ Water	Ambient Air	623/16	Hydrogen	

Chapter 4: Experimental Procedure

4.1 Catalyst Preparation

In this study commercially available CARiACT spherical silica gel pellets (FUJI SILYSIA CHEMICAL LTD, Japan, grade Q-10, 5-10 mesh size, surface are 319 m^2/g) were used as the catalyst support material. The support was first dehydrated in an oven at 450-500 ^oC. The dehydrated silica pellets were saturated with n-heptane solvent. The saturated pellets were then dried at a slow rate to 60-65 ^oC. This ensured that only the external periphery of the gel lost n-heptane.

Cobalt nitrate hexahydrate was used as the metal salt precursor. Depending on the design of experiments (shown in Table 3) the metal salt was either dehydrated at 180-200 ^oC or left as received. To avoid rehydration (where required) the catalyst samples were prepared in a nitrogen glove-box. The dehydrated samples were then placed in ethanol (containing 3 – 4% water by weight), while the hydrated samples were placed in water. The salt-ethanol solution was heated to 70^oC while the salt-water system was heated to approximately 90 ^oC. The hot solution was then poured into a fritted funnel.

Urea was used as the base for precipitation. Urea solution was either made in ethanol or water depending on the system (dehydrated or hydrated). The surface dried pellets were immersed in the hot salt solution, and the urea solution was then added drop-wise. During this precipitation step, the entire mixture was continuously stirred to avoid bulk precipitation. The time of precipitation was adjusted to control the amount of cobalt loaded (around 20% within eggshell). A vacuum pump was used to remove the excess solution. All loaded catalysts were subjected to rapid drying (pressure dropped from zero to 30 in-Hg gauge in one minute) in a vacuum furnace. After drying the samples were

either calcined in air (hydrated samples) or simultaneously reduced/calcined in a packed bed reactor (dehydrated samples). The thickness of the eggshell was based on previous work done by Iglesia et al. [37]. Factors that controlled the thickness of the eggshell included (i) drying rate and temperature during the removal of n-heptane from the gel's outer periphery, (ii) contact time of the gel with the precursor solution during precipitation, and (iii) the rate of vacuum drying. Magnified images of the eggshell catalyst are shown in Figure 7. Table 4 indicates the measured and required thickness of the eggshell.

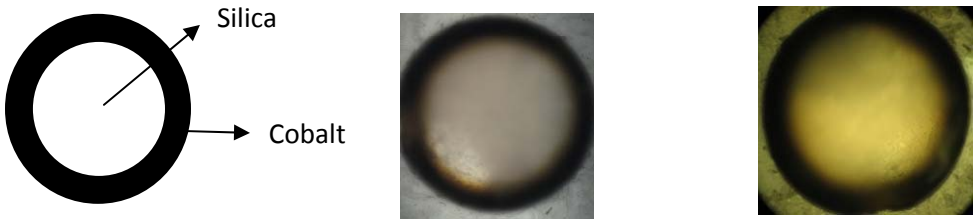

Conceptual diagram Sample-2 Sample-4

Figure 7. Magnified images of eggshell profile obtained using optical microscope

4.2 Experimental Setup

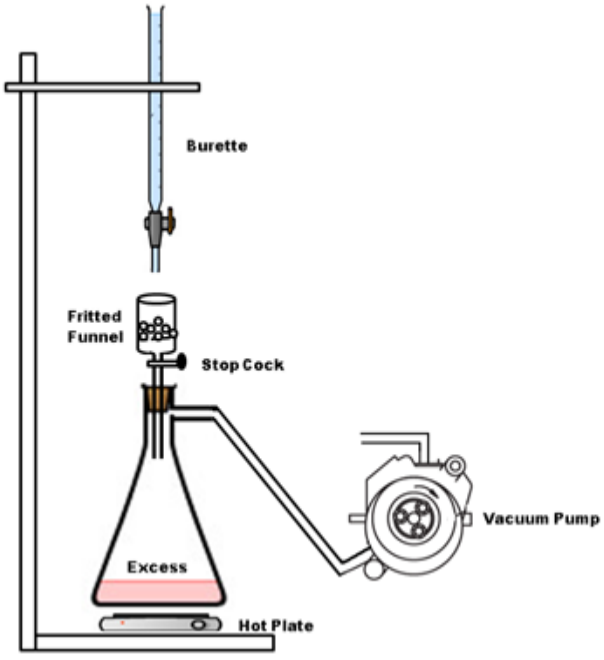

Data

Solution:-

Burette……Urea

Funnel…….Cobalt nitrate

Titration Temperature:-

Aqueous System……90 ^{o}C

Non Aqueous System……70 ^{o}C

Titration Time:-

Aqueous System……1min 20 s

Non Aqueous System……1min 40 s

Figure 8. Experimental setup for catalyst preparation via precipitation

4.3 Catalyst Characterization

An optical microscope was used to determine the thickness of the egg shell. Randomly selected samples were cut in half using a razor blade and then further sliced to get circular cross sections (showing egg shell and silica). Sand paper (600 grit) was used to polish the samples. The eggshell thickness was calculated from magnified images of the 2mm catalyst samples.

In order to characterize the surface and near surface species present on the prepared samples, XPS (X-Ray photoelectron spectroscopy) was carried out in a Perkin Elmer PHI 560 UHV XPS/ SAM system. Sample degassing was performed for 24 hours under 10^{-6} Torr vacuum. XPS elemental analysis was done using both Al Kα and Mg Kα radiation based on the binding energy range and resolution requirement. A "Gaussian Curve Fit" was used to identify the chemical-state and relative concentration of elemental species. References for the binding energies were taken from the Handbook of Photoelectron Spectroscopy [45] and prior research work [8]. Note that XPS is a surface analysis technique limited to 10^{-1} monolayer fractions and is not representative of bulk composition.

N_2-physisorption was performed at -196 ^{o}C using the Quantachrome Autosorb gas sorption system. Each sample was degassed under UHV for 24 hours at 100 ^{o} C. BJH method was applied on the desorption branch of the isotherm in order to calculate the pore volume as a function of pore size. The pore diameter was taken as the one where maximum differential pore volume occurred.

Hydrogen adsorption isotherm was taken on a Quantachrome Autosorb gas sorption unit at 373 K. The samples were reduced in hydrogen at 673 K; the flow of hydrogen was maintained to swiftly remove the water formed during reduction. In situ calcination/reduction samples were directly transferred to the apparatus after drying in a vacuum. Following reduction, the samples were evacuated at 673 K and then cooled down to 373 K. An adsorption isotherm was recorded from 80-560 mmHg (gauge). The

amount of chemisorbed hydrogen was determined by extrapolating the straight-line portion of the isotherm to zero pressure. For calculating dispersion, it was assumed that two cobalt sites were covered by one hydrogen molecule and all the exposed cobalt atoms were reduced to metallic cobalt. Hydrogen chemisorptions provided strong insight into metal support interaction and dispersion. In a way the results of hydrogen chemisorption form the basis of our studies.

Temperature programmed reduction (TPR) was also done in the Quantachrome Autosorb gas sorption unit. The sample was exposed to the reducing gas (pure hydrogen) while the temperature was increased at 5 K/min from ambient to 973 K. The consumption of hydrogen was measured by analyzing the effluent gas with the thermal conductivity detector. By plotting the output signal against the temperature a catalyst reduction pattern was obtained, indicating metal-support interaction and the presence/absence of silicates. TPR results proved useful as they provided in situ results for the hydrogen calcined catalyst.

A Bio-RAD Excalibur FTS3000 FTIR operated in ATR (attenuated total reflectance) mode was used to further characterize the different catalyst samples. For this purpose, a Pike Technologies diamond MIRacle single reflection horizontal attenuated total reflectance (HATR) unit designed for use in FTIR spectrometer was utilized. Two hundred and fifty scans were recorded for each sample at a resolution of 4 cm^{-1} and a sensitivity of 16. A permanently aligned gas cell was used to analyze the effluent gases during Fischer-Tropsch runs. The 60 mm diameter gas cell provided an infrared beam length of 2.4 m and consisted of a borosilicate glass body with a KBr window and a total volume of 0.1 liter.

4.4 Catalyst Testing

The different catalyst samples were tested in a fixed bed reactor (BTRS Jr supplied by Autoclave Engineers) at conventional FTS conditions. Two mass flow controllers by Brooks instrument (Model 5850 EM and EC) were used to control the flow of reactant

gases (CO and H_2) and an Omega flow meter (FMA 1818) was used to monitor the flow of inert gas (N_2), Figure 9. The mixed gases were pre-heated by an oven heater built inside the main assembly. The reactor itself consisted of a 0.43 m SS 316 tube with an internal diameter of 0.013 m, fitted with a jacket heater. In order to monitor the catalyst bed temperature a thermocouple was inserted throughout the length of the bed which was connected to a PID temperature controller. A manual backpressure regulator was used to maintain the system pressure. The catalyst bed consisted of active catalyst mixed with inert quartz chips in the ratio of 1:4 by volume; the total volume of active catalyst was around 6 mL (2.4 g). Different catalyst samples (those calcined in air & those dried, waiting to be in situ calcined) were reduced at atmospheric pressure and 400 ^{o}C in a dynamic hydrogen stream (flow rate = 5 L/min) for 16 hrs. The low thermal conductivity of the bed was the main cause for such a high flow of the reduction gas. The FT reaction was carried out at 200 ^{O}C and 20 bar with H_2/CO ratio of 2:1, once the equilibrium was achieved, WHSV was maintained at 94 g/ ($hr.g_{cat+inert}$) and temperature was raised slowly to approximately 230 ^{o}C. The purpose of the quartz chips was to effectively control the reaction isotherm in the absence of an external cooling mechanism.

CO conversion was calculated using Fourier transform infrared spectroscopy. Absorbance versus concentration plots were developed for the individual gases (carbon monoxide and methane). The following normalized expression was used for CO conversion

$$CO\ conversion\ (\%) = \frac{(moles\ of\ CO)_{in} - (Moles\ \ of\ CO)_{out}}{(Moles\ of\ CO)in} \times 100$$

$$Selectivity\ of\ i\ th\ product = \frac{Moles\ of\ i\ th\ product}{(Moles\ of\ CO)_{in} - (moles\ of\ CO)_{out}} \times 100$$

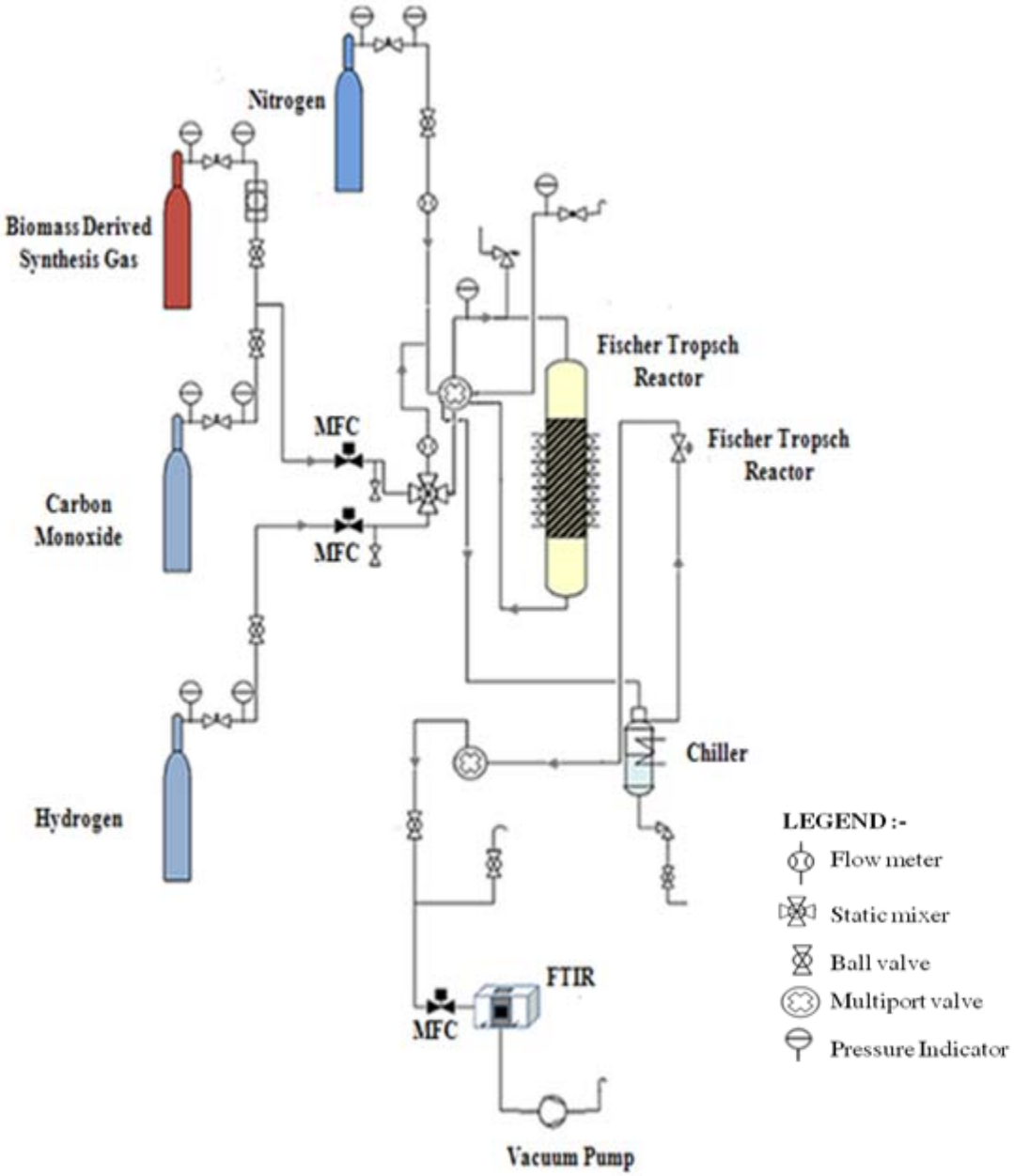

Figure 9. Bench-scale reactor setup for carrying out Fischer-Tropsch synthesis

Chapter 5: Characterization Results and Discussion

5.1 Verification of Eggshell Thickness

Iglesia et al. [37] have identified that the eggshell thickness is related to the cobalt surface density and the pellet's mean pore radius via parameter "χ", as shown below.

$$\chi = (R_o - R_c)^2 \, \theta_M / r_p$$

Where R_o is the pellet radius, R_c is the radius of internal non impregnated core, θ_M is the cobalt site density (atoms /m^2) and r_p is the pore radius. χ is the parameter that strictly depends on the structural properties of the catalyst. Iglesia et al. [37] has suggested that for optimal activity and selectivity of eggshell catalyst, the value of χ must lie between 200 – 2000 * 10^{-16}, (more preferably 100 – 1000 * 10^{-16}). Based on the hydrogen chemisorption results (for θ_M) and the nitrogen physisorption results (for r_p), the optimum eggshell thickness has been calculated and compared with the results from optical microscopy as shown in Table 4.

Table 4. Eggshell thickness of samples prepared under different conditions

Sample ID	**Mean Pore Radius (10^9 *m)**	**Cobalt Density On Surface (10^{17} Co.m^{-2})**	**χ 10^{-16}**	**($R_o - R_c$) Calculated (mm)**	**($R_o - R_c$) Actual (mm)**
Sample 1	6.25	0.53	100-1000	0.47-1.00	0.50
Sample 2	4.75	3.48	100-1000	0.19-0.42	0.25
Sample 3	5.00	5.20	100-1000	0.15-0.34	0.25
Sample 4	6.00	1.80	100-1000	0.26-0.58	0.30

These results show that the required thickness depends on the dispersion. A highly dispersed catalyst (cobalt surface density) requires a smaller thickness which results in the reduction of the overall cobalt loading and cost saving (and vice versa). The thickness of the shell also impacts the product selectivity. As explained by Iglesia [37] the hydrocarbon product selectivity depends on the arrival of the diffusion limited reactant (CO) at the active sites. As more active sites are available for CO adsorption, the probability of chain growth increases (in case of a thin shell). On the other hand, the low inter-pellet concentration increases the required eggshell thickness which favors the formation of lighter hydrocarbons.

The eggshell thickness of all the samples was within the required limits (it is important to note that a random sampling technique has been employed and the reported thickness is based on the analysis of five samples in each case). In line with the above mentioned hypothesis which relates CO adsorption to the number of active sites, the Sample 2, 3 and 4, have produced FTS liquid product in the range of diesel and aviation fuel. This is shown by the GC analysis in Figures 17-19. However, the GC analysis of the Sample 1 (Figure 16) has shifted towards lower hydrocarbons owing to a thicker shell. Apart from eggshell thickness, other factors also influence the product selectivity.

5.2 XPS

The surface and near surface elemental state of all the samples was analyzed by XPS as shown in Table 5. Clearly the sample developed in ethanol and calcined in situ in hydrogen has the highest Co surface content. However, on the other hand, the catalyst synthesized in aqueous media and calcined in air showed the least Co concentration. For characterization these samples were cut in hemispheres and analyzed such that only the top hemispherical section was under the focus of the incident beam. Hence, the analysis is strictly quaitative, however, it indicates the repartition of cobalt ions on silica surface.

Khodakov [2] states that the I_{CO}/I_{Si} ratio represents the dispersion of cobalt ions on a silica surface. In other words higher ratios are characteristic of higher dispersion, while

lower ratios indicate that metal agglomeration has taken place. Table 5 shows the ratio for the different samples, which increases in the following order, Sample 3 > Sample2 > Sample4 > Sample1. Thus, the precursor deposition and decomposition conditions control the active metal distribution on the silica support; however, the degree of impact is different for each case. The effect of the solvent and the precipitation environment is greater than that of the calcinations atmosphere. This is demonstrated by the intensity ratios of Samples 2 and 3 (same precipitation conditions, different calcination environment) verses that between the Samples 3 and 4 (different precipitation conditions).

The precipitation solvent controls the interaction between the salt and the silica surface. This interaction is the basis for the building block that controls metal crystallite distribution on the surface. It was observed that an inert calcination environment during the precursor loading limited rehydration of the silica surface resulting in reduced silica-metal interactions. On the other hand, the calcination environment controls the decomposition of precursor (cobalt nitrate) and the formation of cobalt silicate. It has no impact on the initial interaction developed during the salt deposition. This was consistent with Sample 1 prepared under least favorable theoretical conditions (water as precursor solvent, impregnation in ambient air and calcination in stagnant air) having the lowest intensity ratio.

Table 5. The surface composition of the catalyst based on XPS analysis

Catalyst	**Surface Atom Content (n%)**			n_{Co} / n_{Si}	S_{CO} / S_{Si}	I_{CO} / I_{Si}
	Co	**O**	**Si**			
Sample 1	2.5	70.0	27.5	0.1	10.6	1.1
Sample 2	15.0	66.6	18.4	0.8	10.6	8.5
Sample 3	27.0	62.5	10.5	2.6	10.6	27.6
Sample 4	8.0	66.1	25.9	0.3	10.6	3.2

S= Sensitivity factor; values available in literature [45]

High resolution XPS spectrum of the Co 2p region is shown in Figure 10. The presence of Co_3O_4 is identified by the peaks located in the range of 779.5 to 780.2 eV [45]. In order to confirm this result, decomposition of the Co2p spectrum has been performed using a "Gaussian fit" routine. The feature consists of Co^{III} (octahedral), Co^{II} (tetrahedral) and Co^{II} satellites as shown in Fig 10(b). The binding energies shown in Table 6 are in agreement with available values found in literature [45]. Earnst et al. [8] has found that the area ratios of Co $2p_{3/2}$ peaks of Co^{III} and Co^{II} is around 2 which gives a corresponding formula $Co^{+2}(Co^{+3})_2O_4$.

Comparison of the high resolution spectra (Fig 10(a)) shows a relatively intense satellite structure (787.0 and 803.0 eV) for the Sample 1 and 2. Girardon et al. [46] argue that this is a characteristic of Co^{2+} ions associated with the residual cobalt nitrate. Since, both of these samples were calcined in air, it can be concluded that calcination in static air lead to partial decomposition of cobalt nitrate. This observation is confirmed by the FTIR spectra shown in Figure 13. As motioned earlier, the decomposition in static air is rapid, accompanied by a surge in heat transfer, while the decomposition in hydrogen is gradual with a higher degree of completion.

No mixed metal-support oxides are observed within the first few atomic layers of the outer periphery via XPS analysis. However, bulk techniques are required to identify the extent of any metal support interactions on different samples. For this reason, XRD, TPR and FTIR-ATR were used in this work to access the presence of any metal-support interactions. This interaction can either be in the form of anchors (between salt ions and SiOH) developed during precipitation or in the form of bulk metal-support oxides e.g. orthosilicates, a high temperature product formed in the presence of water. In this research the development of the former has been encouraged while the latter is suppressed to give rise to high dispersion and greater reducibility.

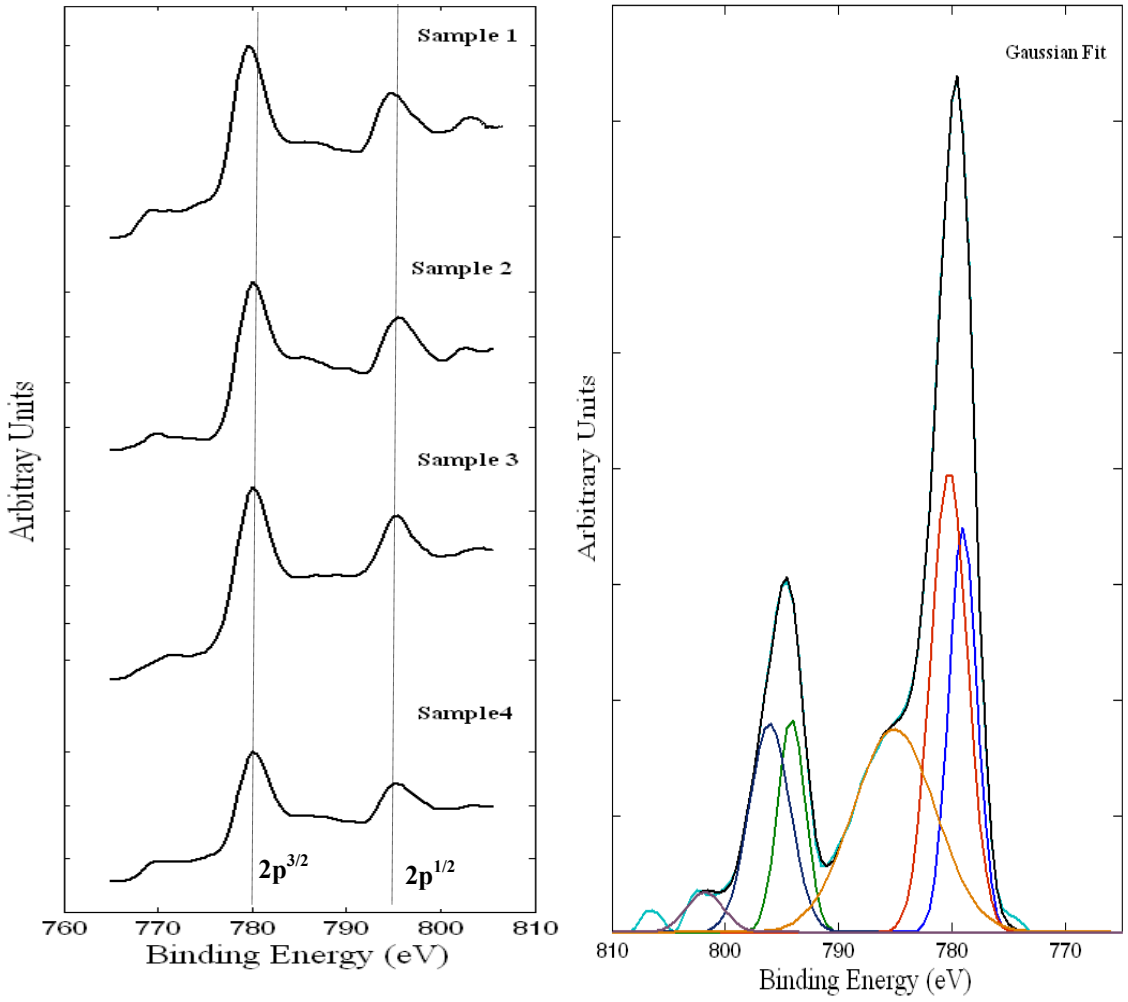

Figure 10. (a) High resolution spectra of the Co2p level of all catalyst samples, (b) decomposition of Sample 2 spectra using Gaussian fit

Table 6. Binding energies and surface contributions by $Co2p^{3/2}$ and $Co2p^{1/2}$. (Fig 10(b))

Catalyst Sample	Binding Energy (eV) $Co2p^{3/2}$			Binding Energy (eV) $Co2p^{1/2}$		
	Co^{+3}	Co^{+2}	Co^{+2} (satellite)	Co^{+3}	Co^{+2}	Co^{+2} (satellite)
Sample-1	780.0	781.0	787.0	795.0	797.0	803.0
Sample-2	780.0	781.5	787.5	795.0	796.5	803.5
Sample-3	780.0	782.5	787.5	795.0	796.5	802.5
Sample-4	779.0	780.5	785.5	794.0	796.0	802.5

5.3 Nitrogen Physisorption

BET surface area measurements are presented in Table 7. The data indicate that the surface area is dependent on the calcination environment and the solvent used. Sample 3, which was synthesized using ethanol as the solvent under a nitrogen atmosphere and calcined in dynamic hydrogen (most favored theoretical route), has retained most of the original surface area (surface area of CARiACT support is 319 m^2/g). However, the presence of water (either as solvent or as moisture in atmosphere) reduces the surface area as shown by the Samples 1 and 4.

It is evident that a transition in the catalyst loading conditions (from ethanol to water and nitrogen to ambient air) changes the surface area by 20% (Sample 3 vs. Sample 4). However, the change in the calcination environment (from static air to dynamic hydrogen) has approximately half the effect (Sample 2 vs. Sample 3). Thus, like the case of active metal distribution, the surface area also depends on precursor loading and decomposition conditions, but the impact of the loading parameters is more significant than that of the calcination conditions.

Pore size distribution plays an important role in selectivity of high molecular weight hydrocarbons. Song and Li [47] state that pore size in the range of 6-10 nm display optimal Fischer-Tropsch activity and higher C_5+ selectivity. CARiACT Q-10 support has mean pore size of around 10 nm (as stated by Fujitech). As shown in Table 7, the presence of water increases the pore size, shifting the mean pore size distribution to higher values. The large pore size reduces the required residence time of gases for chain growth. This relative impact on C_5+ distribution is shown by the gas chromatographic (GC) analysis of the Sample 1 (Figure 16). Samples 2 and 3 have pores within the desirable size range which favors chain growth due to optimum residence time within the pores according to the literature cited. The GC results (Figure 17 and 18) confirm this hypothesis; however, the distribution depends on other factors such as dispersion and eggshell thickness.

Table 7. Surface properties of 20% Co/SiO_2 catalyst based on N_2 physisorption

Catalyst ID	Specific Surface Properties		Pore Size (nm)
	BET Surface Area (m^2/g)	BJH Pore Volume (cm^3/g)	
Sample 1	255.0	1.04	13.0
Sample 2	290.7	0.91	9.5
Sample 3	313.0	1.01	10.0
Sample 4	260.3	0.97	12.0

5.4 Hydrogen Chemisorption

Dissociative hydrogen chemisorption was used for an in depth analysis of metal surface and metal-support interaction. Reuel and Bartholomew [48] have reported that this is an activated process which requires high temperature to ensure irreversibility. Numerous studies show that 373 K (100 ^oC) is the temperature that provides optimum irreversible adsorption [49]. The total hydrogen uptake for different catalyst samples (at 373K) is shown in Figure 11 along with the actual isotherm. The chemisorptive monolayer was obtained by extrapolation to zero pressure.

Total hydrogen uptake in Figure 11(a) represents both the reversible and irreversible uptake. However, since the isotherm was developed at 373 K (optimum for dissociative adsorption), this adsorption trend represents the activity trend of different catalyst samples. Bligaard et al. [3] has shown that the dissociative adsorption on the catalyst surface is the rate limiting step in Fischer-Tropsch synthesis. So, the rate of FTS should vary in the following order: Sample 3 > Sample 2 > Sample 4 > Sample 1. Actual runs under FTS conditions have confirmed this hypothesis as shown in Table 9.

Monolayer volume at zero pressure (extrapolation of the isotherm) determines the surface properties of different samples. These quantitative results not only serve the purpose of comparison but also correlate microscopic properties with catalyst activity.

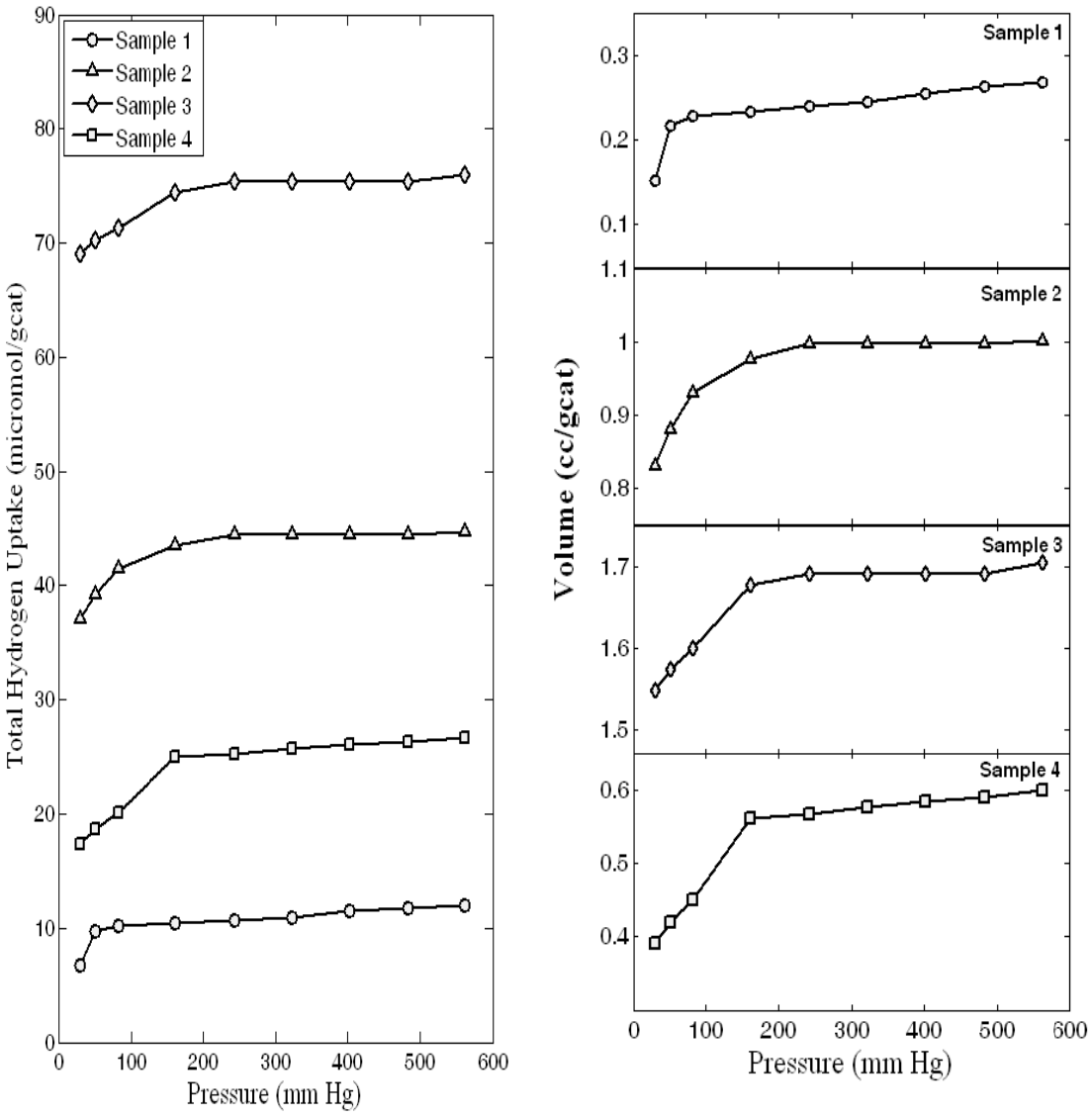

Figure 11. (a) Total hydrogen uptake at 373 K, (b) combined isotherm at 373K

Following formulae are used to calculate the properties of active surface:

- Monolayer Uptake (μ mol/g)

$$N_m = 44.6 \cdot V_m$$

V_m = Monolayer Coverage

- Active Surface Area (m^2/g)

$$ASA = \frac{N_m \cdot S \cdot A_m}{166}$$

= Adsorption Stoichiometry

A_m =Cross-sectional area of each active surface atom

= 6.6 $^oA^2$

- Active Metal Dispersion (%)

$$D = \frac{N_m \cdot S \cdot M}{100 * L}$$

M = molecular weight = 59

L = Percent loading of supported metal

- Average Crystal Size: (Angstrom)

$$d = \frac{C_1}{D}$$

C_1= 94 [50]

The obtained results are shown in Table 8. As hypothesized earlier, wetting pattern by alcohol permits the direct contact of metal and support. This anchorage is responsible for the higher dispersion of catalyst sample 2 and 3, both of which have been fabricated using alcohol as the solvent. As stated by Borg et al. [29] the presence of water during calcinations favors crystal growth and agglomeration. In line with this hypothesis, Sample 2, which was calcined in static air shows lower dispersion than Sample 3 (calcined in dynamic hydrogen). The dynamic hydrogen environment improves segregation of an active metal (as cited earlier) and avoids the thermal sintering due to gradual decomposition of the nitrate salt. All these conditions favor high dispersion. Presence of water in the form of water of hydration on the silica surface, or as a precursor solvent, effectively blocks contact between the precursor and the support. Thus, despite

the favorable calcinations condition, Sample 4 (prepared in aqueous media) shows lower dispersion than Sample 2 (prepared in alcohol). Sample 1, being prepared in water and calcined in air, shows greater agglomeration of active metal evident by large crystal size and low dispersion.

For the case of cobalt/silica catalyst, crystal growth follows an opposite trend to that of dispersion. High support interactions result in reduced agglomeration, and smaller average crystal size. As shown in Table 8, crystal size increases in the following order, Sample 1 > Sample 4 > Sample 2 > Sample 3. Thermodynamic analysis of the catalyst kinetics [51] shows that nano particles in the size range of 6 -11 nm show a maxima in Fischer-Tropsch synthesis activity. In accordance with this hypothesis, Sample 3 is expected to show optimum properties for Fischer-Tropsch synthesis. Conversely, Sample 1 is expected to show minimum conversion.

Table 8. Properties of active metal based on hydrogen dissociative adsorption

Sample ID	**Actual Loading**	**Monolayer Volume** V_m **(cc/g)**	**Monolayer Uptake** N_m **(μ mol/g)**	**Active Surface Area** **ASA** (m^2/g)	**Dispersion** **D (%age)**	**Average Crystal Size** **d (nm)**
Sample 1	16.0	0.2	10.7	0.9	1.0	94.0
Sample 2	10.0	1.0	50.0	4.0	6.0	15.0
Sample 3	10.0	1.7	76.0	6.1	8.9	10.5
Sample 4	10.0	0.6	25.0	2.0	3.0	31.3

.

The results of hydrogen chemisorption are incomplete without estimating the extent of reduction. There is the possibility that interactions between the metal and the support hamper this process. Temperature program reduction (TPR) gives a qualitative measure of the ease of reduction process. Although being qualitative in nature it effectively differentiates between positive metal support interaction (giving rise to high dispersion)

and the irreducible ortho-silicates. TPR results confirm the hypothesis for calcination environment when viewed in conjunction with the hydrogen chemisorptions results.

5.5 Temperature Program Reduction

Temperature program reduction is a valuable technique for evaluating the extent of reduction. The reducibility of a supported cobalt catalyst depends on the preparation condition, reduction conditions, the promoter and the choice of support [4]. Presence of strong metal support interaction can also impact the reduction process; if the interaction exists to the extent that hydro silicates are formed, the reduction process can extend up to 1100 K. However, under normal conditions supported and unsupported Co_3O_4 spinal follows a two step reduction process as shown below [52].

$$Co_3O_4 + H_2 \longrightarrow CoO + H_2O$$

$$3CoO + 3\,H_2 \longrightarrow 3Co + 3H_2O$$

During TPR two distinct, but slightly overlapping peaks are usually observed. These peaks can individually be assigned to the two step reduction process if their hydrogen consumption ratio is around 1/3 (stoichiometric ratio). However, deviations have also been observed especially in the case of bimodal particle distribution [8] in which, individual peaks represent reduction of a certain collection of particle sizes.

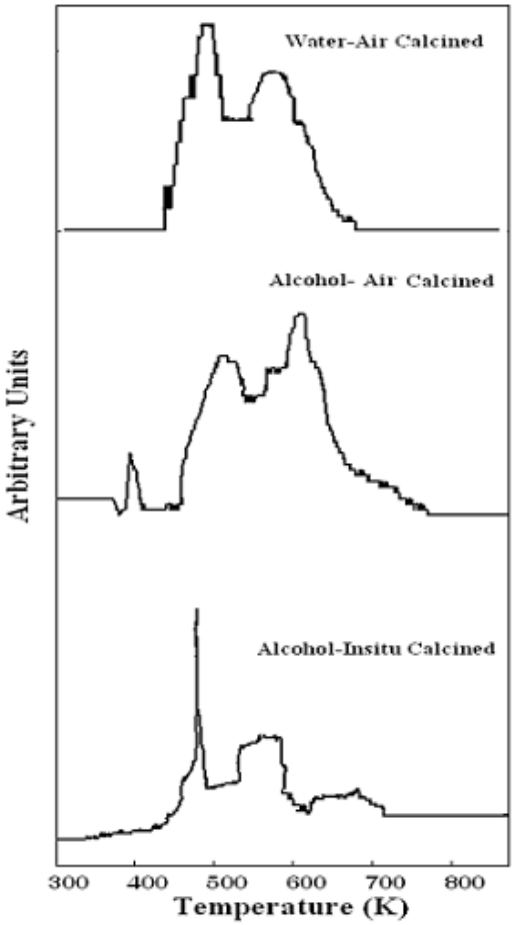

Figure 12. Temperature program reduction. Ramp rate= 5 K/min

Figure 12 shows the TPR of the different catalyst samples. Due to the tight control of parameters during precipitation deposition, the possibility of bimodal particle distribution has been ignored. Steen et al. [6] have extensively studied the reduction profile of different catalyst samples prepared by varying the solvents, the silica supports, the degree of cobalt nitrate dehydration, the drying time and the calcination temperature. They assign the following temperature range for reduction of different species; 540-560 K for reduction of trivalent to divalent cobalt, 570-620 K for reduction of divalent with hardly any interaction with carrier, and around 700-770 K for species with very strong interaction with the support surface. Formation of the cobalt silicates leads to broad reduction peaks ranging between 800 – 1100K.

The TPR profile of Sample 1 shows the first peak centered at 500 K while the second distinct peak has a maxima at 580 K. These peaks represent the two step reduction process with an area ratio of 0.35 relative to each other. Castner et al. [53] reports that stabilization of the oxide phase due to metal support interaction results in broadening of the second peak. Thus, the narrow second peak of Sample 1 (as compared to that of Sample 2), represents a lesser interaction between the metal and the support. In comparison to Sample 2 and 3 there is also a shift in the entire spectrum of Sample 1 towards lower temperature. This shift is also reported to be a measure of metal-support interaction [54].

These results confirm that the presence of water during precipitation-deposition prevents direct contact of the active metal with the silica surface. However, the presence of water during calcination may form some bulk metal-support oxides. However, the impact of loading conditions is much stronger than that of calcination environment. Hydrogen chemisorption results are in line with TPR results, Sample 1 shows strong agglomeration and a very low dispersion, an indicator of low metal support interaction.

The TPR spectrum of Sample 2 shows a small peak at around 400K, this represents decomposition of residual cobalt nitrate. As discussed earlier, the XPS spectrum of this sample shows a strong satellite peak which has already been attributed to the non-

decomposed nitrates. The second and third peak centered at 520 and 610 K represents the two step reduction process with an area ratio of 0.38. The broadening of second peak well beyond 750 K indicates a relatively strong metal support interaction. In fact the instrument limitation restricts analysis to 873K, preventing the identification of any cobalt silicates.

The use of ethanol permits interaction of the metal and the support due to its specific attachment on the silica surface. This is confirmed by the broadening of the second TPR peak. During the calcination in static air there is a possibility of forming irreducible oxides as well as that of agglomeration (cited earlier). The working limitations restrict experimental observation; otherwise one may have observed a peak at around 1070 K attributed to hydro silicates. Hydrogen chemisorptions results confirm the increase in dispersion and the decrease in crystal size as compared to Sample 1 indicative of enhanced interactions. However, as compare to Sample 3, the dispersion is low, due to agglomeration caused by rapid heat surges and insufficient removal of calcinations product in static air.

TPR results of Sample 3 look remarkably different from other two catalysts analyzed. As this catalyst is only vacuum dried, the sharp peak appearing at around 480K represents the decomposition of nitrate ions. During the preparation of the catalyst, cobalt nitrate salt is dehydrated at around 180 ^{o}C, it is possible that some cobalt oxides are formed at that high temperature. Thus, the two relatively small peaks correspond either to the reduction of those oxides or to the reduction of intermediate products formed during nitrate decomposition. Previous studies show that under nitrogen and hydrogen glow discharge plasma, cobalt nitrate on alumina decomposes at low temperature producing very fine oxide crystals [2]. The TPR profile of Sample 3 is following the same trend i.e. the decomposition temperature is much lower than that of a typical calcination temperature (i.e. 673K) and produces small crystallites, as shown in Table 8. TPR spectra of Sample 4 (not shown here) consist of nitrate decomposition peak at approximately same temperature (that sample is also in situ calcined in hydrogen). The two smaller peaks are also present but they are shifted to a lower temperature. This shift can be

attributed to the use of water as a solvent that diminishes metal support contact. As a result the dispersion goes down but reduction process becomes easier.

5.6 Fourier Transform Infrared Spectroscopy

In order to confirm the qualitative results of temperature program reduction and gain a thorough insight into the nature of surface interaction and the formation of cobalt silicate, IR spectra of various samples were obtained. Based on the previous research work [55], following are IR visible, vibration by silica at 1100, 975, 800 cm^{-1}, by nitrate ions at 1610, 1365, 842 cm^{-1} , by hydroxyl groups at 1640 cm^{-1} , and by Co_3O_4 at 667 cm^{-1} . CoO is known to be IR inactive specie.

As shown in Figure 13, the IR spectra contain ordered variation that depends on the preparation and treatment conditions of various samples. In order to elucidate the impact of loading, a pre-calcined portion of Sample 3 (synthesized in alcohol) has also been included. The IR spectrum of sample 3 shows vibration bands at around 670 cm^{-1}. This peak either represents Co_3O_4 (produced during the dehydration of cobalt nitrate) or Co-O associated with $Co(OH)_2$ produced during titration with urea [56]. At around 800 and 1100 cm^{-1} peaks corresponding to Si-O are visible.

An interesting feature has appeared around 1030 cm^{-1} which corresponds to Si-O-Co bond formed as indicated in previous research work [31]. As stated earlier, the use of alcohol during loading on dehydrated and partially dehydroxylated silica permits the direct contact of cobalt with the support surface. Such a contact gives rise to Si-O-Co bonding. Two visible peaks around 1320 and 1610 cm^{-1} corresponds to the nitrate ions present on the surface of the dried catalyst. Additionally there are two low intensity peaks centered around 1420 and 1500 cm^{-1}. Literature survey has revealed that NH_4^+ ions have an absorption region of 1390-1485 cm^{-1} corresponding to deformation [57]. Therefore these two peaks correspond to the ammonium ion formed during the urea decomposition. However, XPS analysis did not reveal the presence of any nitrogenous specie on the surface of the catalyst.

Sample 2 gives a spectrum similar to the dried catalyst. This sample was prepared in alcohol and calcined in air. As shown by the XPS high resolution spectrum of sample 1 and 2, the nitrate ions are not entirely decomposed in static air. The IR spectra confirm this finding, by showing the vibration bands around 1320 and 1610 cm^{-1}. Presence of Co_3O_4 on the surface is confirmed by the vibration band at around 640 cm^{-1}. As expected from its broad TPR peak (well beyond 700 ^oC), presence of metal support interaction is confirmed in the sample by a feature appearing at around 1020 cm^{-1}. However, it is important to identify the subtle difference in the nature of Si-O-Co peak that appears in the dried sample and the air calcined sample. As, discussed earlier, the metal support interaction at the time of salt deposition is essential to develop a building block for high dispersion. On the other hand, calcination in static air keeps the product (including water) in contact with the surface for a longer period of time. In the presence of migrating silica, the presence of water can result in the formation of cobalt silicate, a product that severely reduces the catalyst reducibility. However, without a TPR features at around 1000-1100 K it is not possible to differentiate the two. Si-O absorbance peak is visible at 800 and 1100 cm^{-1}. The presence of NH_4^+ ion is confirmed by a single peak centered at around 1420 cm^{-1}, additional proof of incomplete decomposition in static air.

Nitrate peaks are missing in the spectrum of Sample 3 due to complete decomposition in dynamic hydrogen which is consistent to what has been observed in the XPS high resolution spectrum. No cobalt silica interaction is observed. This is very interesting as it seems that the dynamic hydrogen may cause a surface rearrangement that retains the high dispersion of cobalt crystallites (as evinced by chemisorptions results of the Sample3), but diminishes the coordination between the cobalt and the silica (i.e. Si-O-Co). The Co_3O_4 peak at 670 cm^{-1} is more intense owing to the presence of small crystallites (also shown in hydrogen chemisorptions results). The silica peaks at 800 and 1100 cm^{-1} are also more pronounced. A new peak has appeared at around 1650 cm^{-1}. Previous research work [31] associates this peak to silanol groups (SiOH) on the silica surface. It is hypothesized that in situ calcination has cleansed the surface as a result unassociated silanol groups have become visible.

Since both Sample 1 and 4 were prepared in aqueous medium, it is hypothesized that there is little to no possibility of a direct contact between the metal and the support. Thus, the Si-O-Co interaction peak is not present in the IR spectra. This promotes the agglomeration as shown by a low dispersion of samples 1 and 4. The complete decomposition of the precursor is evident for the Sample 4 (calcined in situ in hydrogen) due to the disappearance of vibration peaks associated to the nitrates and the ammonium ions. However, Sample 1 shows a smaller peak centered at 1350 and another one at 1500 cm^{-1}. The Co-O coupled vibration (associated to Co_3O_4) is relatively more intense for Sample 4 due to the smaller crystal size when compare to Sample 1. The presence of silanol groups in Sample 4 is indicated by the peak at 1650 cm^{-1}, it is more intense with respect to that of Sample 3.

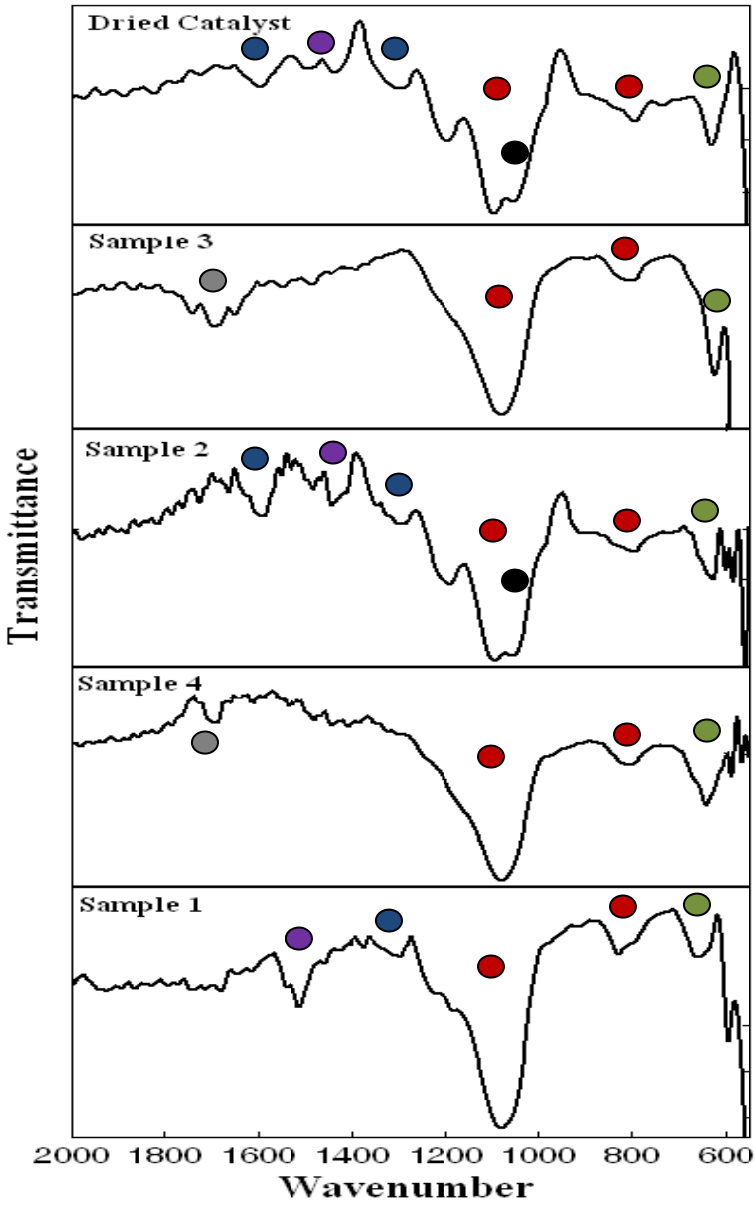

Figure 13. Infrared spectra of catalysts using attenuated total reflectance (ATR)

Chapter 6: Catalyst Performance

6.1 Activity Measurement Using Research Grade Gases

In order to assess the performance of different catalyst samples, FTS has been conducted for 72 hrs in a fixed bed reactor (detail of which has been explained earlier). The performance parameters are given Table 9; all parameters have been evaluated after 24 hrs at which time steady state is assumed. As shown in Table 9, Sample 3 exhibits the highest CO conversion. This can be explained in part by the dissociative hydrogen adsorption results given in Table 8, where Sample 3 shows the highest concentration of active metal on the surface (i.e. dispersion). This high active surface area provides more reaction sites and aids in the chain growth. The opposite holds true for Sample 1. Based on the "χ" requirement an alternate explanation can also be provided. Sample 1 has the thickest "eggshell", this reduces the number of sites available per m^2 surface area for the diffusion limited reactant i.e. carbon monoxide for a given percentage of loading (especially when the dispersion is low). While, in the case of Sample 3, the active metal is concentrated at the outer periphery, being more accessible to carbon monoxide. This results in higher conversion at relatively low loading. The activity of samples 2 and 4 follow the expected trend based on their surface properties i.e. Sample 2 > Sample 4. The impact of pore size on the selectivity is evident; Samples 2 and 3 have a mean pore size within the desirable range of 6-10 nm, thus they provide optimum inter-pellet residence time for chain growth as shown by the C_{5+} selectivity. However, the mean pore size of the samples 1 and 4 are greater than 10 nm. Within the pores of these samples, the reactant and products have a less residence time than optimum which retards chain growth. The use of cobalt as an active ingredient keeps CO_2 production in check. So, despite low temperature (around 503 K), water gas shift reaction does not proceed to an appreciable degree in all cases.

The variation of activity for all the catalyst samples has been studied; Figure 15 shows CO conversion as a function of time. The CO conversion shows a gradual increase for the first 20-24 hrs. This is attributed to the decrease in the supply of inert nitrogen gas. Nitrogen is initially supplied to suppress catalyst sintering. Usually at around 24 hrs, the catalyst bed is filled with liquid product which significantly improves the heat transfer across and along the bed and diminishes the risk of sintering. Another shift in conversion is observed around 40-45 hrs, this is due to the adjustment in CO/H_2 ratio from 1/3 to 1/2 as required by stoichiometry. It is interesting to note that the gradual rise for the first 20-24 hrs is more than that observed at 40-45 hrs. This can be due to the filling of pores with hydrocarbon liquid which blocks the active sites preventing further hydrogenation [31]. Sample 4 shows anomalous behavior during the first 24 hrs as conversion essentially remained constant. In general activity follows the adsorption trend shown in Figure 11 i.e. Sample 3 > Sample 2 > Sample 4 > Sample 1.

The impact of metal support interaction (MSI) can be correlated with activity. Sample 2 exhibited the presence of cobalt silicates during the time of its preparation. Also during actual runs silicates form in the presence of water, so their concentration increases as the run time progresses. These silicates are responsible for the drop in activity of Sample 2 after 60 hrs of continuous operation. On the other hand, samples 1, 3 and 4 shows relative constant activities. For samples 3 and 4 one can attribute the sustained activity to the in situ treatment in hydrogen.

Table 9. Catalytic performance of cobalt-silica supported catalysts in FT synthesis

Catalyst ID	**Activity hr^{-1}**	**CO conv. (%)**	**Selectivity (%)**		
			C_{1-4}	**CO_2**	**C_{5+}**
Sample 1	1.3	55.0	38.2	11.6	50.1
Sample 2	2.5	73.0	31.1	8.2	60.0
Sample 3	2.8	85.0	27.8	9.2	63.0
Sample 4	1.8	63.0	27.4	15	57.5

Reaction condition 2 MPa, 503 K, WHSV = 94 h^{-1}
Activity: Gram hydrocarbon product/ gram catalyst used per 1 h operation

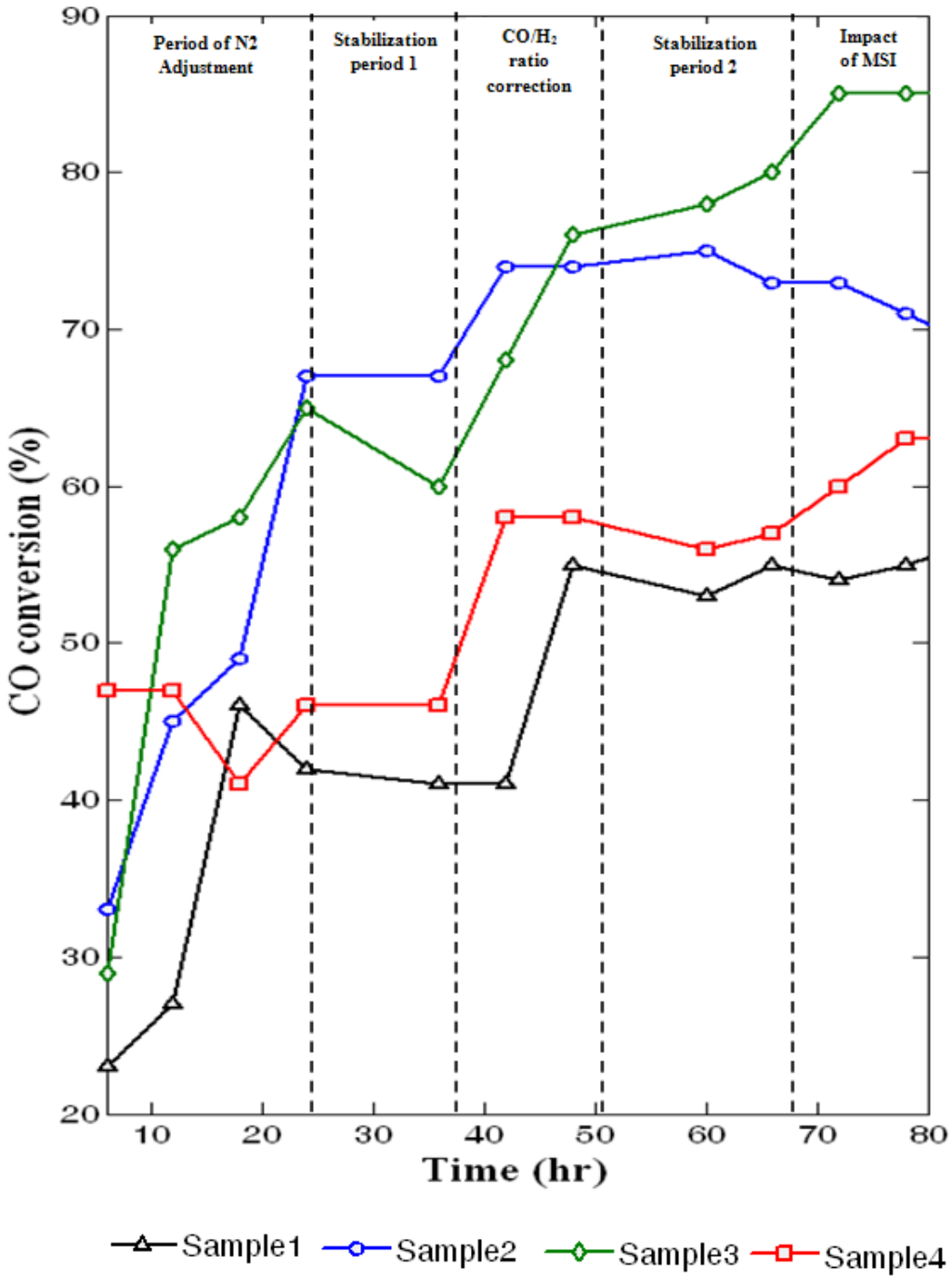

Figure 14. CO conversion with time. Reaction conditions: 2 MPa, 503 K, WHSV= 94 h^{-1}, FTS time: 80 h

6.2 Selectivity Assessment Using Research Grade Gases

The interest in an eggshell profile for FTS has developed due to an ever growing demand for a product specific catalyst and reduced metal loading. Such a catalyst will tremendously reduce the operating cost which would otherwise be required for additional refinement. The product selectivity is fine tuned using a so called "χ" parameter (discussed earlier). This parameter has a strong bearing on the activity of the catalyst as well.

As shown in Table 4, the calculated thickness of the egg shell (based on "χ") depends on the surface concentration of cobalt crystallites. Sample 1, due to lesser per m^2 active metal concentration, requires thicker shell (for a given loading) to ensure the availability of "a sufficient amount" of sites for chain growth and activity. However, carbon monoxide being the diffusion limited reactant may not effectively reach the sites located deep inside the pores, resulting in chain termination at low carbon numbers. This is confirmed by the shift in GC profile of Sample 1 towards lower hydrocarbons. Sample 3 has the highest dispersion and its shell thickness lies around the mean of the desired limit. All these parameters provide a suitable condition for tight control on hydrocarbon product distribution. This is confirmed by the narrow GC profile within the diesel and aviation fuel range. For samples 2 and 4 the thickness of the shell is closer to the lower limit. This favors the formation of longer hydrocarbon chains. As compare to Sample 2, Sample 4 has lesser dispersion; as a result products shift towards higher hydrocarbons as seen in Table 4.

Based on the above discussion, the selectivity of the product depends on the thickness of the eggshell, which in itself is a function of active metal dispersion. This kind of correlation is of immense importance in modern catalysis, a product specific synthesis is highly beneficial especially for the development of alternate energy industry e.g. conversion biomass to liquid fuels. If the refining cost of the fuel is reduced, the alternate energy route becomes economically more feasible.

6.3 Selectivity Assessment Using Biomass Derived Synthesis Gas

The performance of Sample 3 has also been assessed with biomass derived synthesis gas. This gas has been produced by a "Pearson Biomass Reformer", a tubular free flowing hollow reactor which uses crushed pine chips as the primary feed stock. The gasifier outlet gas has the following composition; 30% H2, 30% CO, 30% CH_4 and 10 % CO_2, it is supplied in pressured cylinders for the liquefaction process.

The FTS reaction was carried under normal conditions, however, the additional hydrogen was provided in order to bring CO and H_2 ratio to 1:2, The hydrocarbon product is essentially free of sulfur (around 0.5 ppm). This clean green fuel has strong market demand especially in the aviation industry. The produced fuel has a cloud point around -40 ^{o}C, which is much lower than conventional biodiesel, and the gravimetric energy is also higher than ethanol making it a preferential alternate fuel. It is important to note that Sample 3 is tunable based on its eggshell thickness, thus it can meet customer specific demands based on ever-changing market conditions.

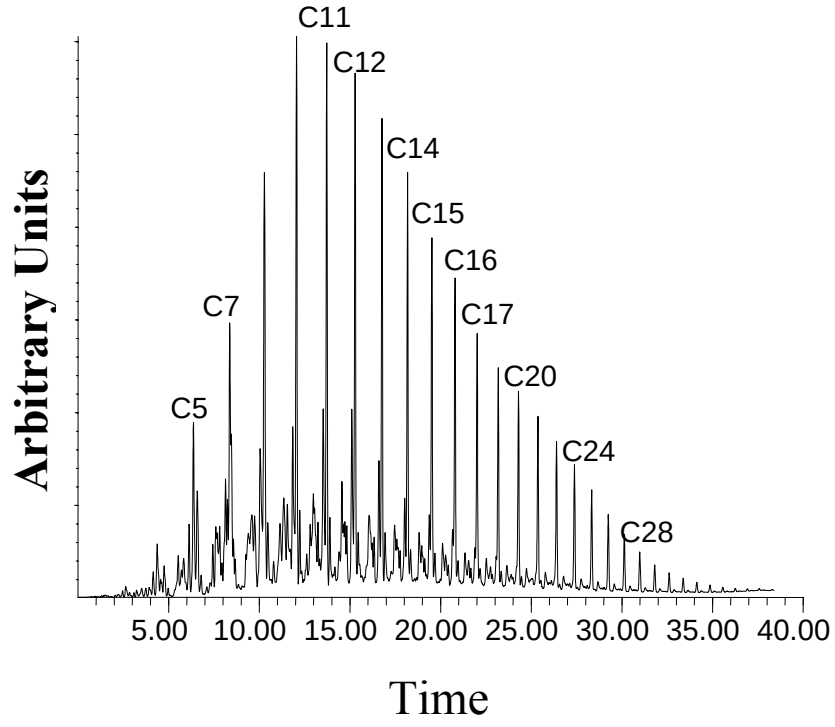

Figure 15. GC analysis of liquid product obtained from FTS of Sample 1

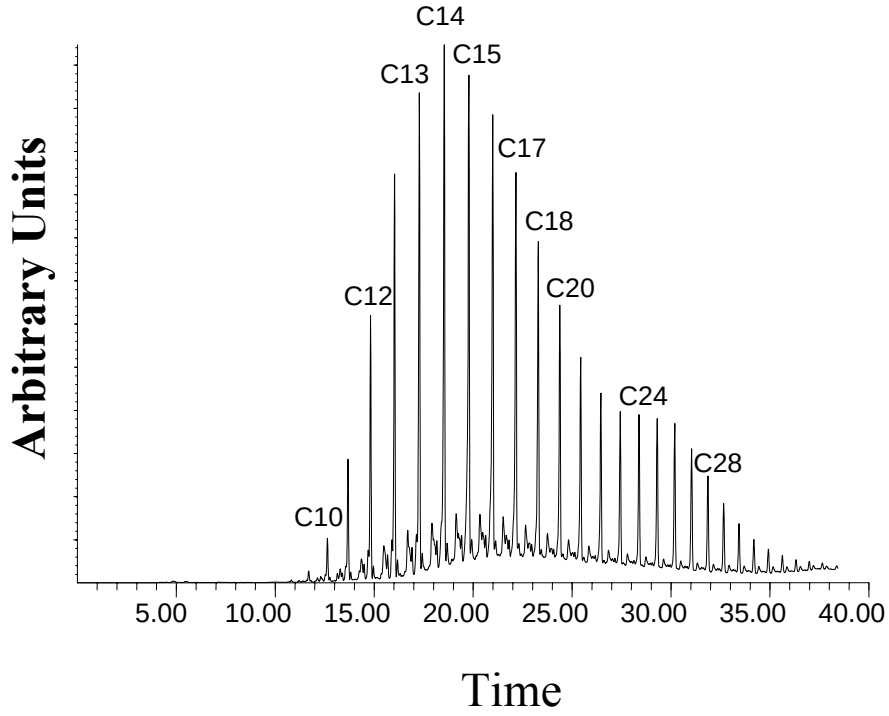

Figure 16. GC analysis of liquid product obtained from FTS of Sample 2

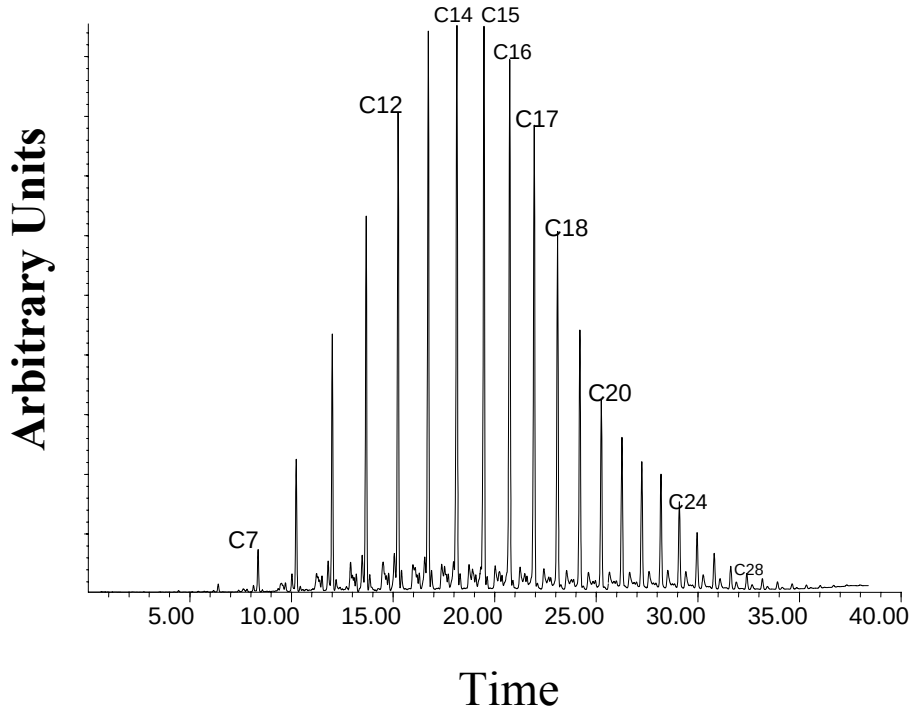

Figure 17. GC analysis of liquid product obtained from FTS of Sample 3

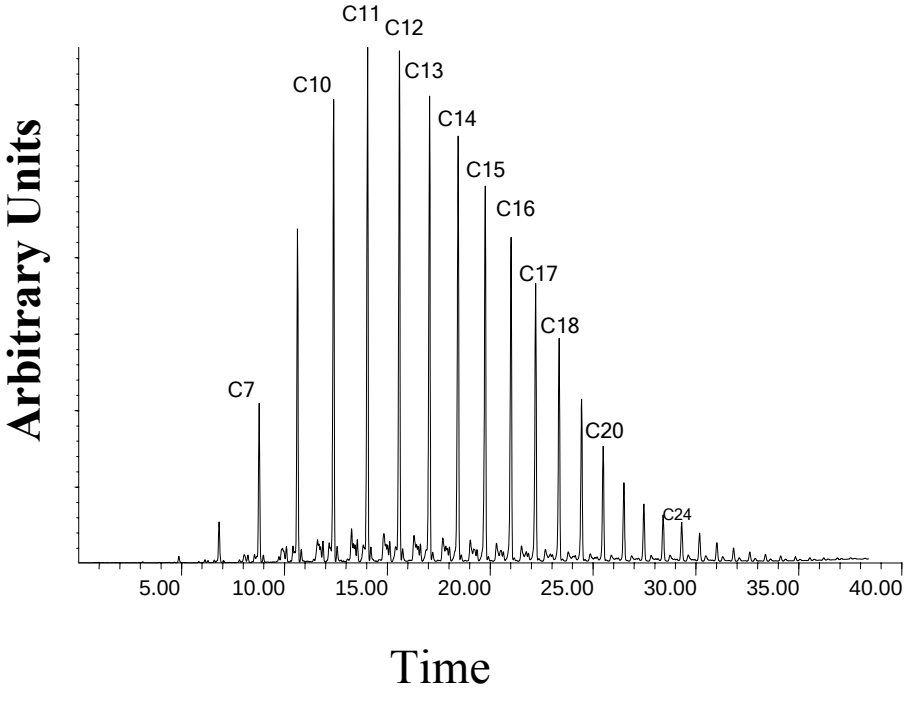

Figure 18. GC analysis of liquid product obtained from FTS of Sample 4

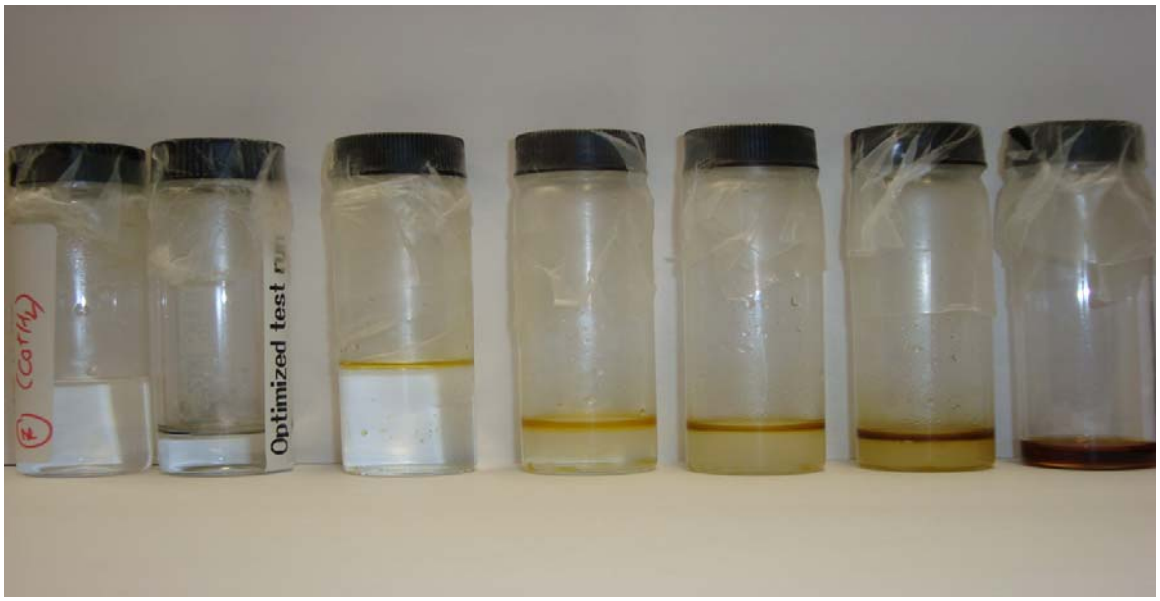

Figure 19. Random samples of FTS liquid product produced from the developed catalysts

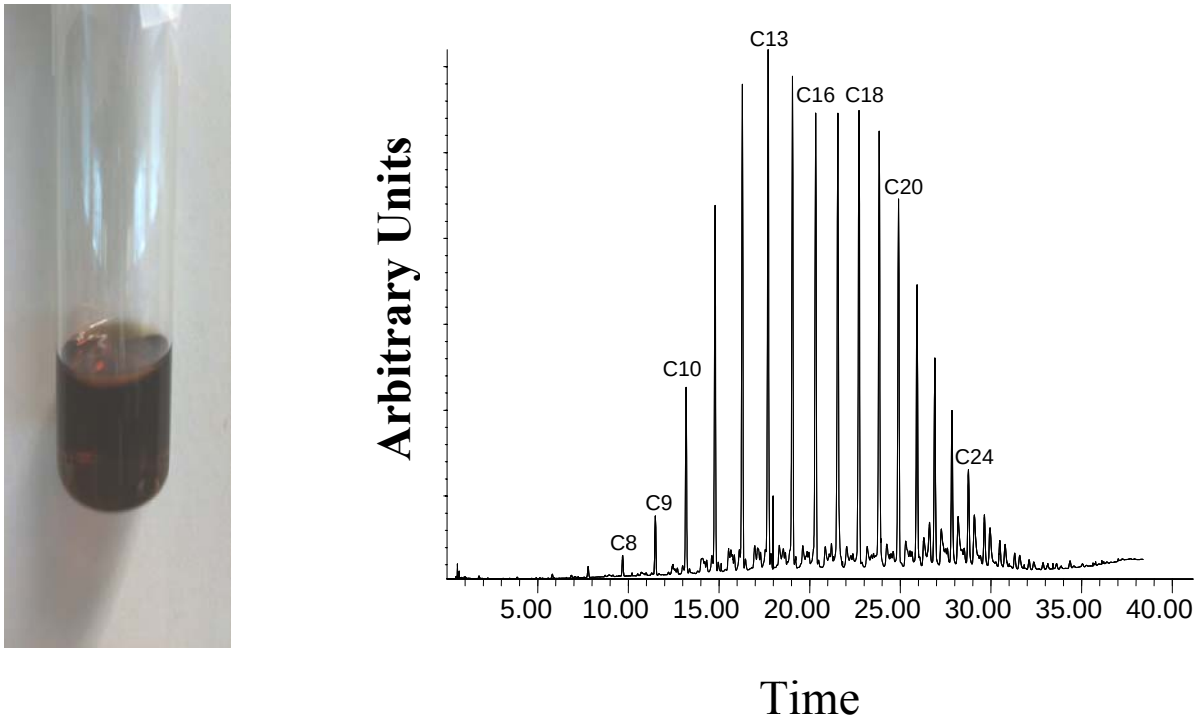

Figure 20. (a) Biomass derived liquid fuel sample, (b) result of third party GC analysis

Chapter 7: Discussion of Experimental Findings

7.1 Metal Deposition in an Aqueous Medium

Under ambient conditions, a silica surface is covered with immobilized single or multiple layers of water molecules. This is due to the strong affinity of different types of silanol groups towards water molecules via hydrogen bonding. It is very difficult to have a direct interaction between the silica surface and a foreign molecule in the presence of this layer. Therefore, in this study the silica gel pellets were heated to around 500 ^{o}C, under this condition the silica surface loses all the water of hydration and approximately half of its silanol groups.

This thermally treated silica gel posses both the hydrophobic and the hydrophilic properties. Thus, upon soaking in the non-polar n-heptane, these pellets absorb a sufficient amount of this solvent. After drying, these pellets were transferred to an aqueous salt solution; both the water and the salt compete for the attachment to silica surface. At the start, the pH of the aqueous paste (salt & water; 1 g/mL) is around 3.0 which is closer to the silica gel's isoelectric point. This neutral surface has strong affinity for water and forms an immobilized aqua layer. There is no direct contact between salt and the silica surface. The penetration depth of the solution within the pores depends on the availability of the dried surface area essentially free of n-heptane.

The dropwise addition of aqueous urea solution in the cobalt nitrate solution at 95 ^{o}C during precipitation increases the pH to 5 via the following decomposition reaction [26]

$$CO(NH_2)_2 \longrightarrow NH_3 + HNCO$$

In an acidic aqueous environment HNCO is converted to CO_2, and ammonia reacts with proton to give NH_4^+ [26].

$$HNCO + H^+ + H_2O \longrightarrow NH4^+ + CO_2$$
$$NH_3 + H^+ \longrightarrow NH_4^+$$

Both these reactions consume H^+ which leads to an increase in the pH. Under such conditions Co^{2+} forms hydroxide [26]. If the surface has exposed silanol groups these hydroxides undergo an ion exchange with the surface and creating direct contact between SiO^- and Co^{2+}. However, due to the low pH at the start, these silanol groups are covered with water before any ion exchange can take place. So the cobalt will adsorb above this stagnant water layer in the form of $Co_X(OH)_Y(NO3)_Z$ .w(H2O) [26].

7.2 Metal Deposition in a Non-Aqueous Medium

Since the initial treatment of the silica gel is the same as it was in the case of aqueous solution, the same theory applies here. However, the interaction of ethanol with the silica gel at the time of immersion is very different than that of water. As discussed earlier roughly half of the available silanol groups will be covered by the alcohol leaving the rest for the solute ions. The initial pH of the cobalt nitrate-ethanol system is around 2.5 and contains 3% water, by weight. This amount of water is sufficient for the ionization of the cobalt nitrate, but, the silica surface does not have a charge. Under this condition these cobalt ions will swarm near the silica surface (kept in thermal motion by phonons) without any direct contact.

The drop wise addition of the urea-ethanol solution in the cobalt nitrate solution at 70 ^oC will results in partial thermal decomposition of urea [26] as shown below.

$$CO(NH_2)_2 \longrightarrow NH_3 + HNCO$$

However, due to the presence of ethanol, some ethyl carbamate will also form via following mechanism [59]

$$CO(NH_2)_2 + CH_3CH_2OH \longrightarrow CH_3CH_2OCONH2 + NH_3$$

In the presence of water HNCO is converted to CO_2, and ammonia reacts with proton to give NH_4^+ [26].

$$HNCO + H^+ + H_2O \longrightarrow NH4^+ + CO_2$$
$$NH_3 + H^+ \longrightarrow NH_4^+$$

These reactions increase the pH of the system to ~ 4.0. Due to this rise in pH, the silica surface becomes negatively charged and undergoes coordination covalent bonding with the swarming cobalt ions. However, only a fraction of the available silanol groups will ionize; this promotes dispersion and avoids agglomeration. This bonded cobalt-silica structure serve as the base for a highly dispersed building block of metal crystallites.

7.3 Calcination in the Stagnant Air

Calcination in stagnant air is a complex process that involves the decomposition of the salt precursor. This decomposition pathway depends on the calcination media and the temperature. Sietsma et al. [33] have proposed the decomposition of $Ni_3(NO_3)_2(OH)_4$ at 450 ^oC in terms of $Ni(NO_3)_2$. According to Sietsma, the overall process is explained by the following reaction.

$$Ni(NO_3)_2\,(s) \longrightarrow NiO\,(s) + 2\,NO_2\,(g) + \tfrac{1}{2}\,O_2\,(g)$$

Based on these finding, the following decomposition reaction is proposed for the air calcined cobalt samples.

$$3\,Co_X(OH)_Y(NO_3)_Z \longrightarrow x\,Co_3O_4 + 3z\,NO_2 + 3/2\,y\,H_2O + (3/2\,z + 3/4\,y - 2x)\,O_2$$

No CoO peak is observed by XPS or XRD analysis. Also TPR analysis has shown two reduction peaks assigned Co^{2+} and Co^{3+}. All these findings confirm that only Co_3O_4 is formed during the calcination process.

In stagnant moist air this water remains in contact with the surface and reacts back to form cobalt hydroxide. As discussed earlier, this cobalt hydroxide further reacts with migrating silica to form cobalt-silicate. This hypothesis is confirmed by the FTIR spectra of Sample 2. However, no silicates are observed in the spectrum of Sample 1. This is due to the initial deposition of the salt in the stagnant aqua layer. In the absence of a strong interaction with the silica surface, the metal precursors are loosely absorbed on the immobilized water layer, very close to each other. Decomposition in air is accompanied by a rapid thermal surge. This heat flux promotes the agglomeration of cobalt crystallites which are already under thermal motion and in close proximity. No significant surface rearrangement is observed in this case.

7.4 Calcination in the Dynamic Hydrogen

Calcination-reduction is carried out in the hydrogen gas is a gradual and slow process with uniform heat transfer. Since dried catalysts are directly subjected to the hydrogen treatment, they will first undergo the decomposition reaction. Sietsma et al. [33] identified that treatment of $Ni(NO_3)_2$ in an oxygen scavenging atmosphere . They have not observation the formation of oxygen during this reaction. Since hydrogen is also an oxygen scavenger, we can deduce a parallelism between the two mechanisms.

The decomposition of $Ni(NO_3)_2$ proceeds as follows [33]

$$Ni(NO_3)_2(s) + NO \longrightarrow NiO(s) + 3NO_2(g)$$

Based on this reaction, the following decomposition reaction is proposed for the cobalt nitrate precursor developed in an aqueous solution.

$$3Co_X(OH)_Y(NO_3)_Z + (-4x+3/2y+3z)\,H_2 \longrightarrow xCo_3O_4 + 3z\,NO_2 + (-4x+3z+3y)\,H_2O$$

However, the catalyst precursor synthesized in ethanol may contain some unionized cobalt nitrate. If such is the case decomposition in hydrogen will proceed as follows

$$3Co(NO_3)_2 + 2H_2 \longrightarrow Co_3O_4 + 6NO_2 + 2H_2O$$

Co_3O_4 further reduces to metallic cobalt via the two step reduction process, explained in the TPR analysis. The two small peaks in the TPR analysis of Sample 3 confirm the formation of Co_3O_4. However, it cannot be conclusively stated whether any CoO is formed during the decomposition or not. Since the decomposition in dynamic hydrogen leads to the formation of water, space velocity of the gas must be kept high. This avoids the formation of irreducible cobalt silicate.

Due to the non-availability of complete data for $Co_X(OH)_Y(NO_3)_Z$ complex, one cannot compare the heat of formation data for the two calcination processes. This data can reveal the amount of heat a surface absorbs during the decomposition and is suggested for future work. It is suspected that in the stagnant air, the surface absorbs more heat, than in the case of hydrogen. This added heat contributes to crystal growth and agglomeration.

Treatment in hydrogen is suspected of causing some surface rearrangements. This is confirmed by the FTIR spectrum of the dried catalyst and the spectrum of the Sample 3 (Figure 13). The dried catalyst (developed in a non-aqueous solution) shows the presence of cobalt-silica interaction. However, when the catalyst is treated in the hydrogen, this interaction is unobservable. This may be the result of hydrogen incorporation within the silica structure or some other form of rearrangement. In order to confirm this hypothesis we need sophisticated characterization techniques such as scanning tunneling microscopy and/or neutron scattering is required.

Chapter 8: Conclusions

A highly active and selective FTS Co/SiO_2 eggshell catalyst has been developed using hydrophobic-hydrophilic interactions between n-heptane and ethanol (or water). Active Co metal has been impregnated in the silica support either under ambient conditions using aqueous cobalt nitrate solution or under nitrogen atmosphere using cobalt nitrate-alcohol solution. Synthesis of an active catalyst requires a balance of strong interaction between the active metal and support without formation of irreducible mixed metal support oxides. Calcination atmosphere also impacts the final redistribution of active metal on support. Presence of water in the calcination environment enhances metal-support interaction. Silanol groups on silica can alter morphology and dispersion of active metals on the support. Solvents used for precursor such as water or alcohol attach to these silanol sites in specific configuration and compete with metal salts during ion exchange and adsorption. By fine tuning the solvent attachments on heat treated silica we have fabricated a cobalt/silica catalyst with high dispersion. Silica has affinity for both polar and non-polar molecule depending on the surface conditions. This property is exploited in preparing an eggshell profile. Simultaneous calcinations/reduction in dynamic hydrogen environment was used to further enhance the dispersion and reducibility. The parameter "χ" from previous work [37] is adopted in order to evaluate catalyst performance.

Catalyst samples synthesized in water did not show significant metal-support interactions and when calcined in air, undergo significant sintering. This sintering reduces their active surface area and dispersion, and the average crystal size increases significantly. The samples synthesized in ethanol show considerable cobalt-silica interactions during the initial loading. When thermally treated in stagnant air, irreducible cobalt silicates are formed in these samples. The formation of silicates significantly decreases their degree of

reduction. The ethanol, stagnant air samples exhibited an increased dispersion and relatively smaller crystal size than the water, stagnant air samples. On the other hand, thermal treatment of these non-aqueous samples in a dynamic hydrogen environment produces very fine crystallites and no irreducible cobalt- silicates.

For a given loading, the thickness of the eggshell required for optimum selectivity and activity is dependent on the dispersion of the active metal.. The lower the dispersion, the greater the thickness required in order to ensure the availability of requisite sites (for high activity and desired selectivity). On the other hand, a highly dispersed catalyst achieves the required activity and selectivity within a narrow eggshell.

Eggshell thickness has a direct impact on product selectivity. Carbon monoxide is the diffusion limited reactant and its dissociation is the rate limiting step in Fischer-Tropsch Synthesis [3]. By exploiting this fact and synthesizing a catalytic system with low dispersion and a thick eggshell, the diffusion limited arrival of carbon monoxide is reduced to all active sites. This results in an early termination of hydrocarbon chain growth in the range of gasoline and aviation fuel. While, a thinner eggshell and high concentration of active sites promotes chain growth. However, due to the selected range of "χ" the overall distribution lies within narrow hydrocarbon cut. The activity of a catalyst depends on its dispersion and reducibility. The change in solvent and calcination atmosphere varies the catalyst activity. However, the relative impact of solvent is more than that of calcination atmosphere. The catalyst activity pattern parallels the dispersion, i.e. high dispersion gives more conversion. Product selectivity has been controlled by eggshell thickness; current focus is in the production of diesel and aviation fuel. Gas chromatograph analyses of the resulting liquid fuel products show a very narrow hydrocarbon distribution

References

1. *World Energy Outlook 2004.* Retrieved from http://www.iea.org/textbase/nppdf /free /2004/weo2004.pdf , International Energy Agency, Paris, 2004, p. 29.
2. A. Y. Khodakov, *Braz. J. Phys.* 39, 171 (2009).
3. T. Bligaard et al., *J. Catal*. 224, 206 (2004).
4. A. Y. Khodakov, W. Chu, P. Fongarland, *Chem. Rev.* 107, 1692 (2007).
5. E.Iglesia, S. C. Reyes, R. J. Madon, S. L. Soled, *Adv. Catal.* 39, 221 (1993).
6. E. van steen et al., *J. Catal.* 162, 220 (1996).
7. S. W. Ho, M. Houalla, D. M. Hercules, *J. Phys. Chem.* 94, 936 (1990).
8. B. Earnest, S. Libs, P. Cahumette, A. Kiennemann, *Appl. Catal. A* 186, 145 (1999).
9. W. Stober, *Beitr. Silikose-Forsch.* H-89, 87 (1966).
10. D. E. Meyers, N. Hackerman, *J. Phys. Chem*. 70, 2077 (1966).
11. M. M. Dubinin, B. P. Bering, V. V. Serpinski, *Recent Progress in Surface Science*, Academic, New York, 1964, p. 42.
12. L. D. Belyakova, O. M. Dzhigit, A. V. Kiselev, *Zh. Fiz. Khim*. 31, 1577 (1957).
13. K. R. Lange, *J. Colloid. Sci.* 20, 231 (1965).
14. R. L. Dalton, R. K. Iler, *J. Phys. Chem.* 60, 995 (1956).
15. K. Kleir, A. C. Zettlemoyer, *J. Colloid Interface Sci*. 58, 216 (1977).
16. J. H. De Boer, J. M. Vleeskens, *K. Ned. Akad. Wet. Proc. Ser. B*, 60, 23 (1957).
17. C. G. Armistead, J. A. Hockey, *Trans. Faraday Soc*. 48, 58 (1974).
18. G. J. Young, *J. Colloid Sci.* 13, 67 (1958).
19. M. L. Hair, W. Hertl, *J. Phys. Chem.* 73, 4269 (1969).
20. C. Clark-Monks, B. Ellis, *J. Colloid Interface Sci*. 44, 37 (1973).
21. L. Robert, *C. R. Acad. Sci.* 234, 2066 (1952).
22. R. K. Iler, *The Chemistry of Silica*, John Wiley and Sons, New York, 1979, p. 689
23. R. K. Iler, *The Chemistry of Silica*, John Wiley and Sons, New York, 1979, p. 690

24. R. K. Iler, *The Chemistry of Silica*, John Wiley and Sons, New York, 1979, p. 663
25. T. W. Healy, R. O. James, R. Cooper, *Advance in Chemistry Series 79,* American Chemical Society, Washington, D.C., 1968, p. 62.
26. M. Rajmathi, P. V. Kamath, *Int. J. Inorg. Mater.* 3, 901 (2001).
27. R. Matmaan et al., *J. Phys. Chem.* 72, 97 (1968).
28. D. L. Dugger et al., *J. Phys. Chem.* 68, 757 (1964).
29. O. Borg et al., *Top. Catal.* 45, 39 (2007).
30. Puskas et al., *Appl. Catal. A.* 311, 146 (2006).
31. A. H. Kababji, B. Jospeh, J. T. Wolan, *Catal. Lett.* 130, 72 (2009).
32. B. Linyang et al., *Catal. Commun.* 10, 2013 (2009).
33. J. R. A. Sietsma et al., *J. Catal.* 260, 227 (2008).
34. K. E. Coulter, A. G. Sault, *J. Catal*. 154, 56 (1995).
35. J. M. Jablonski, M. Wolcyrz, L. Krajczyk, *J. Catal.* 173, 530 (1998).
36. Z. Tao et al., *Catal. Lett.,* 117, 130 (2007).
37. E. Iglesia et al., *J. Catal.* 153, 108 (1995).
38. M. F. Post et al., *AIChE J*. 35, 1107 (1989).
39. E. Peluso et al., *Chem. Eng. Sci.* 56, 1239 (2001).
40. E. Iglesia et al., *Top. Catal.* 2, 17 (2005).
41. M. Nele et al., *Appl. Catal.*178, 177 (1999).
42. M. K. Niemela et al., *Top. Catal.* 2, 45 (1995).
43. C. H. Bartholomew, R. J. Farrauto, *Fundamental of Industrial Catalytic Processes,* John Wiley and Sons, New Jersey, 2006, p. 98.
44. C. H. Bartholomew, R. J. Farrauto, *Fundamental of Industrial Catalytic Processes,* John Wiley and Sons, New Jersey, 2006, p. 95.
45. J. F. Moulder, W. F. Stickle, P. E. Sobol, K. D. Bomben, *Handbook of X-ray Photoelectron Spectroscopy*, Physical Electronic Inc, Eden Prairie, 1992, p. 83.
46. J. S. Giradon et al., *J. Catal.* 248, 143 (2007).
47. D. Song, J. Lee, *J. mol. Catal. A* 247, 206 (2006).
48. R. C. Reuel, C. H. Bartholomew, *J. Catal.* 85, 63 (1984).
49. C. H. Bartholomew, *Catal. Lett.* 7, 27 (1990).

50. C. H. Bartholomew, R. J. Farrauto, *Fundamental of Industrial Catalytic Processes*, John Wiley and Sons, New Jersey, 2006, p. 83.
51. D. Y. Murzin, *Chem. Eng. Sci.* 64, 1046 (2009).
52. A. M. Hilmen, D. Schanke, A. Holmen, *Catal. Lett.* 38, 143 (1996).
53. D. G. Castner, P. R. Watson, I. Y. Chan, *J. Phys. Chem.* 94, 819 (1990).
54. L. Zeng-xi et al., Chin. *J. Process Eng*. 6, 656 (2006).
55. I. Puskas et al., *Appl. Catal. A* 316, 197 (2007).
56. *NIST Standard Reference Database Number 69*, Retrieved from http://webbook. nist. gov/chemistry/.
57. H. Gunzler, G. Han-Ulrich, *IR Spectroscopy*, Wiley-VCH, Weinheim, 2002.
58. *Reference Library*, XPert HighScore, PANanlytical B. V, Almelo.
59. D. Wang, D.Yang, X. Zhai, L. Zhou, *Fuel Process. Technol*. 88, 807 (2007).